Japan). The mice were kept in a 12-hour light/12-hour dark cycle with free access to food and water. The mice were randomly assigned to three experimental groups: left thoracotomy under mechanical ventilation (THX group), left pneumonectomy under mechanical ventilation (PNX group), or 9-week-old male mice without any interventions (CON group).

The mice were anesthetized with 100 mg/kg of ketamine and 10 mg/kg of xylazine administered subcutaneously. They were intubated with an 18-gauge catheter and connected to a rodent ventilator, adjusted to maintain a respiratory rate of 100 breaths/minute, 10-ml/kg tidal volume, 2 cm H_2O positive end-expiratory pressure, and 0.21 inspired oxygen. A 20-mm long posterolateral skin incision was made, followed by thoracotomy in the fifth intercostal space with dissection of the serratus anterior and a latissimus dorsi muscles. In the THX group, thoracotomy was closed without pneumonectomy. In the PNX group, the whole left lung was resected from the pleural cavity. The left main bronchus with left pulmonary artery and vein were ligated at the hilum with 5–0 silk before removal of the lung. The tidal volume was reduced from 10 to 6 ml/kg after the lung was removed. The fifth intercostal space was closed with a single surgical suture, and the skin and muscle incisions were closed with two sutures to avoid excessive tension on the muscles. The duration of mechanical ventilation for the whole surgical procedure was approximately 10 min in both groups. All mice recovered quickly after termination of mechanical ventilation and were promptly extubated. The mice were weighed and were observed daily for any signs of distress or changes in behavior. The mice were killed at respective time points by injection of 100 mg/kg of ketamine and 10 mg/kg of xylazine, followed by exsanguination from the inferior vena cava.

All experimental protocols were reviewed by the Committee on the Ethics of Animal Experiments at the School of Medicine, Keio University, and were performed in accordance with Guidelines for Animal Experiments issued by the School of Medicine, Keio University Experimental Animal Center.

Cell Line

A mouse lung epithelial cell line, MLE12 (CRL-2110, American Type Culture Collection, Manassas,VA), was used to evaluate the efficacy of TTF-1 silencing oligonucleotides. This cell line is known to express TTF-1 (13). The cells were maintained in Dulbecco's medium: Ham's F12, 50:50 mix, supplemented with insulin (0.005 mg/ml), transferrin (0.01 mg/ml), sodium selenite (30 nM), hydrocortisone (10 nM), β-estradiol (10 nM), *N*-2-hydroxyethylpiperazine-*N*′-ethane sulfonic acid (10 mM), l-glutamine (2 mM), and 2% fetal bovine serum, under 5% CO_2.

Western Blot Analysis for TTF-1

For TTF-1 Western blot analysis, the right lung was resected at respective time points, blotted dry, immediately snap frozen in liquid nitrogen, and stored at −80°C. Western blot analysis for TTF-1 protein was performed according to a standard protocol. Briefly, lung tissue was lysed with a denaturing RIPA buffer (Sigma, Stockholm, Sweden), the lysate was centrifuged at 14,000 rpm for 15 minutes at 4°C, and the supernatant was mixed with Laemmli buffer and applied to sodium dodecyl sulfate–polyacrylamide gel electrophoresis gels. The proteins were separated by 12.5% sodium dodecyl sulfate–polyacrylamide gel electrophoresis under reducing conditions and then transferred to poly vinylidene di fluoride (PVDF) membrane for 90 minutes at 90 V using HorizBlot system (ATTO, Tokyo, Japan). After blocking nonspecific reactions with Block Ace (Dainippon Pharmaceutical, Osaka, Japan), the primary antibody for TTF-1 (H-190; Santa Cruz Biotechnology Inc., Santa Cruz, CA) or antibody for β-actin (Abcam, Cambridge, UK) were incubated with the blot overnight at 4°C. The secondary anti-rabbit IgG, ECL anti-rabbit IgG horseradish peroxidase linked with whole antibody (GE Healthcare, UK), was incubated with the blots for 1 hour at room temperature. Bands were detected by enhanced chemiluminescence using ECL Western blotting detection reagents (Amersham Bioscience Corp Buckinghamshire, UK). Band densitometry was quantified using Image J (NIH, Bethesda, MD). Values were normalized to β-actin.

Histological Analyses

For histological analyses, the right lung was inflated with intratracheal instillation of 10% buffered formalin at a pressure of 20 cm H_2O. The trachea was tied under pressure, and the lung was fixed in the chest cavity for 48 hours before removal. Total right lung volume was measured from the fixed specimen by volume displacement as described by Scherle (14), and was normalized to the body weight as lung volume index (LVI). The lung tissue was then embedded in paraffin, and cut sagittally in 4-μm sections. Hematoxylin and eosin staining was done for morphological analyses. Light microscopic morphometric techniques were applied, and the alveolar surface area per unit of lung volume (SVw) was measured as previously described by Weibel (15) and Kawakami and colleagues (16). Briefly, a standard line of the same length (LT) was drawn on the field, and intersections with this line were counted (Iw). SVw was calculated as SVw = 2 Iw/LT. Alveolar duct area was traced and calculated using Image J. Morphologically, alveoli were identified as polyhedral, cup, or wedge-shaped terminal air spaces with discrete septae, whereas terminal, somewhat elongated air spaces from which alveoli emerged were considered as alveolar ducts (17). Five fields were analyzed per animal in four animals.

Immunohistochemistry for TTF-1 and Ki-67 was performed as follows. The primary antibodies used were: anti–TTF-1 rabbit polyclonal antibody (5 μg/ml: clone H-190) and anti–Ki-67 rabbit monoclonal antibody (10 μg/ml: clone SP6; LabVision, Fremont, CA). Secondary antibodies used were: anti-rabbit Ig Immpress (Vector Laboratories, Burlingame, CA) for both. Then they were visualized with 3, 3′-diaminobenzidine (DAB) (Sigma). Nuclei staining positive were counted and expressed in proportion to the number of nuclei in alveolar septal cells. For further analysis, we subgrouped the alveolar septal cells into cells associated with the alveolus (AL), the alveolar duct (AD), or the septal structure protruding into the alveolar duct (ADS), respectively (Figure 2A). Double-staining for TTF-1 and prosurfactant protein C (proSPC) was performed as follows. Anti-proSPC rabbit polyclonal antibody (5 μg/ml: ab28744; Abcam, Cambridge, MA) was used as the primary antibody. Anti-rabbit Ig Immpress and DAB were also used as described above. Thereafter, the sections were rinsed in 1 M glycine-hydrochloric buffered solution for 2 hours. Then the incubation with anti–TTF-1 antibody and was done by ALP-ABC system: biotinylated goat anti-rabbit IgG (Nichirei Bioscience, Tokyo, Japan) and ALP conjugated Strept ABC complex (Dako, Glostrup, Denmark). The final product was visualized Fast Red Substrate Kit (Nichirei).

For each analysis, one section was randomly selected per animal, and five 200-fold magnification fields were randomly selected per section. The slides were coded and masked for identity and were examined by Y.T. and E.I.

Lung Dry Weight Measurements

The lung dry weight in proportion to body weight, lung dry weight index (LDWI), was measured as a gross assessment of compensatory lung growth. The resected lungs were completely dried in a vacuum drying oven (DP22; Yamato Scientific, Tokyo, Japan) at 95°C, and at −270 cm H_2O for 48 hours, and then were weighed.

Knockdown of TTF-1 by Small Inhibitory RNA

Five TTF-1–silencing small inhibitory RNA oligonucleotides, si#1 through si#5, were synthesized and purified by Invitrogen (Carlsbad, CA). Briefly, single-strand RNA was synthesized by the phosphoramidite method. After synthesis of single-strand RNA, RNA was deprotected in two steps from base and phosphate protecting group and 2′-hydroxyl function protecting. Single-strand RNA was desalted or purified after deprotection. The single-strand RNA was annealed as siRNA. By Western blot analysis using MLE 12 cells, oligonucleotides si#2, and si#4 were found to be effective (data not shown). Sequences of si#2 and si#4 were (5′-UUGAAACGUCGCUCGAGCUCGUACA-3′) and (5′-GCUACAAGAUGAAGCGCCGGCUAA-3′), respectively. As control nonsilencing oligonucleotide (nonsi), stealth RNAi negative control duplex (Invitrogen) was used. Each inhibitory RNA was administered intranasally as previously reported (18) using surface active material, cationic cardiolipin analog (CCLA)-based liposome (NeoPharm, Inc., Waukegan, IL). Thirty-five milligrams per kilogram of si#2, si#4, or nonsi were administered into the nasal orifices using a microliter pipetter mixed with CCLA as a total of approximately 25 μl. The administration was done approximately 30 minutes after extubation in both thoracotomy (THXsi#2, THXsi#4, and THXnonsi groups) and pneumonectomy (PNXsi#2, PNXsi#4, and PNXnonsi groups), at which time the mice had sufficiently recovered breathing but were still im-

mobilized. The right lung was resected for histology and protein analyses as described.

RNA Isolation and Reverse Transcription-Polymerase Chain Reaction

Total RNA was isolated by using Isogen (Nippon Gene, Tokyo, Japan) from the residual right lung 12 hours after left pneumonectomy and subsequent administration of TTF-1 siRNAs (#2, #4) or nonsilencing oligonucleotide. Reverse transcriptase–polymerase chain reaction (PCR) for mouse TTF-1 mRNA was performed as described previously (19). The PCR oligonucleotide primers used were 5′-GAGCTGCCTGACGGCC AGGT-3′ (forward) and 5′-TACTCCTGCTTGCTGATCCA-3′ (reverse) for β-actin, and 5′-AACAGCGGCCATGCAGCAGCAC-3′ (forward) and 5′-CCATGTTCTTGCTCACGTCC-3′ (reverse) for TTF-1.

The PCR was performed in 50 mM KCl, 10 mM TRIS, pH 8.3, 1 mM dNTP, 0.5 mM each primer, 5% dimethyl sulfoxide, 2 units Taq DNA polymerase, and $MgCl_2$ (1.5 mM for β-actin, and 1.0 mM for TTF-1). The PCR conditions were 94°C for 5 minutes for 1 cycle followed by 30 to 40 cycles of 94°C for 1 minute, 56°C for 1 minute, 72°C for 1 minute, with a final extension cycle of 72°C for 7 minutes. The products of these reactions were resolved by gel electrophoresis on 2% agarose gels and stained with ethidium bromide.

Statistical Analysis

Data are expressed as mean ± SD. Comparisons between groups were done using Mann-Whitney *U* test (StatView; Abacus, Berkeley, CA). Body weight was compared within groups using paired *t* test (StatView). Other comparisons within groups were done using Mann-Whitney *U* test because the animals were killed for respective time point measurements. *P* values less than 0.05 were considered to be significant.

RESULTS

TTF-1 Protein Expression was Increased Promptly and Transiently in the Right Lung after Left Pneumonectomy

Western blot analysis showed that TTF-1 protein expression in the right lung was increased in the PNX group in comparison with the THX group. This tendency was observed as early as 1 hour, was most significant at 12 hours, and then was diminished beyond 24 hours (Figures 1A and 1B). TTF-1 protein expression in the THX group was not significantly different in comparison with the CON group. Analysis by immunohistochemistry showed that within the PNX group, TTF-1–positive alveolar septal cells were increased significantly at 12 hours (Figure 2A). Double staining for TTF-1 and proSPC at 12 hours in the PNX group indicated that TTF-1–positive cells were also proSPC positive (Figure 2B). The overall proportion of TTF-1–positive alveolar septal cells gradually decreased after 12 hours to the level close to the CON group by 48 hours, although statistical significance was still present (Figure 2C). This tendency was similar in AL, AD, and ADS cells, but the magnitude of increase in comparison with the CON group seemed to be most prominent in the AD cells (Figures 2D–2F). These results indicated that there was a prompt and temporary up-regulation of TTF-1, presumably in the type II alveolar cells in the right lung after left pneumonectomy, and that this up-regulation appeared to be predominant in the AD cells.

In the Residual Right Lung after Left Pneumonectomy, LVI Increased Immediately, after an Increase in LDWI

The body weight of the mice was reduced in the PNX and THX groups, in comparison with the CON group at 24 and 48 hours. Although statistically significant, the difference was 7% at most (Figure 3A). The decreased body weight in the PNX and THX groups was regained from 3 days. The body weight of the mice did not differ significantly between the PNX group and the THX group throughout the experiment period. Therefore, it was considered feasible to compare weight-based indices between these groups.

On gross appearances of the fixed specimens, the residual right lung in the PNX group seemed to be larger than the right lung in the CON group at 48 hours (Figure 3B). Based on the TTF-1 expression data, we examined the macroscopic changes in the right lung after left pneumonectomy focusing primarily on the early phase of compensatory lung growth. Residual right LVI was increased significantly in the PNX group in comparison with the THX group as early as 1 hour after left pneumonectomy (Figure 3C). Within the PNX group, this increase in residual right LVI continued until 7 days but leveled off beyond 7 days. There was no significant change within the THX group during this period, and no significant differences between the THX group and the CON group. In contrast to the changes in LVI, residual right LDWI did not increase significantly in the PNX group in comparison with the THX group until 48 hours (Figure 3D). Beyond 48 hours, this increase continued within the PNX group until 7 days and then leveled off beyond 7 days. Residual right LDWI in the PNX group at 7 days was not statistically different from the total LDWI (right plus left) in the CON group (Figure 3E). There were no significant changes in right LDWI within the THX group during this period, and no significant differences in the right LDWI between the THX group and the CON group. These results suggested that initially there was right lung expansion as early as 1 hour after left pneumonectomy, followed by compensatory lung growth, which became apparent by 48 hours and progressed until approximately

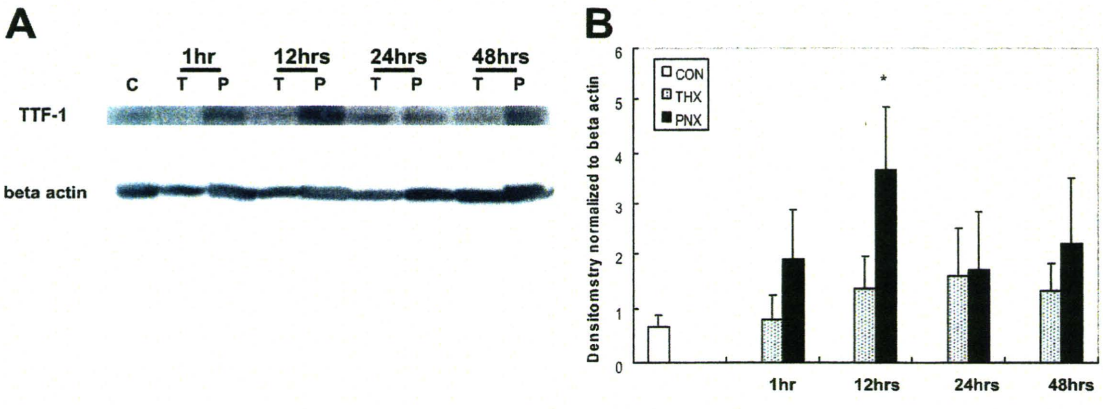

Figure 1. Thyroid transcription factor 1 (TTF-1) protein expression by Western blot analysis in the right lung after left pneumonectomy (PNX group), left thoracotomy (THX group), or no intervention (CON group). (*A*) TTF-1 expression was increased in the PNX group (P) in comparison with the THX group (T) and the CON group (C). (*B*) Densitometry values were normalized to β-actin. TTF-1 expression was increased in the PNX group (n = 4 for each time point) in comparison with the THX group (n = 4 for each time point), and the CON group (n = 4). Statistical significance was seen at 12 hours. **P* = 0.02 versus CON and THX at 12 hours.

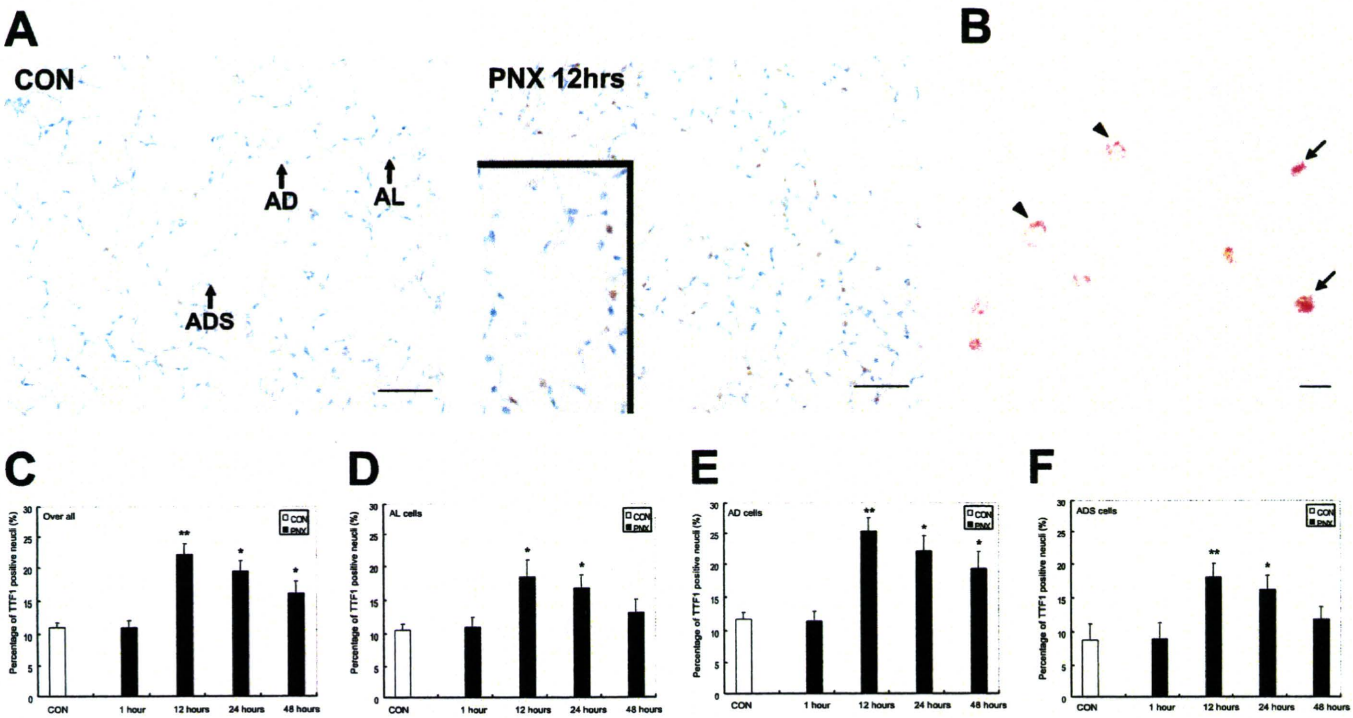

Figure 2. The presence and proportion of thyroid transcription factor 1 (TTF-1)-positive nuclei was evaluated by immunostaining in the right lung after left pneumonectomy (PNX group), or no intervention (CON group). (*A*) TTF-1–positive cells were prominent at 12 hours in the PNX group by immunohistochemistry. For further analysis, the alveolar septal cells were subgrouped into cells associated with the alveolus (AL), the alveolar duct (AD), or the septal structure protruding into the alveolar duct (ADS), as represented. Inset shows TTF-1–positive nuclei in the PNX group, primarily in AD cells (scale bars, 100 μm). (*B*) Double staining for TTF-1 and prosurfactant protein C (proSPC) at 12 hours in the PNX group indicated that TTF-1–positive cells were also proSPC positive. TTF-1 was identified by red-colored nuclei, and proSPC by brown-colored granules in the cytoplasm. Cells positive for both TTF-1 and proSPC are indicated by *arrows*, whereas TTF-1–negative but proSPC-positive cells are indicated by *arrowheads* (scale bar 10 μm). (C) Within the PNX group (n = 4, 20 fields for each time point), the overall proportion of TTF-1–positive alveolar septal cells was increased significantly at 12 hours, after which it was gradually decreased to the level close to the CON group (n = 4, 20 fields) by 48 hours. $^{*}P < 0.0001$ versus CON and PNX 1 hour; $^{**}P < 0.0001$ versus all other measurements. This tendency was similar in (*D*) AL cells, $^{*}P < 0.0001$ versus CON and PNX 1 hour; (*E*) AD cells, $^{*}P < 0.0001$ versus CON and PNX 1 hour; $^{**}P < 0.0006$ versus all other measurements; and (*F*) ADS cells, $^{*}P < 0.01$ versus CON and PNX 1 hour. $^{**}P < 0.01$ versus all other measurements. The magnitude of increase in comparison with the CON group seemed to be most prominent in the AD cells.

7 days, at which time the residual right LDWI in the PNX group matched the total (right plus left) LDWI in the CON group.

Alveolar Duct Area in the Right Lung Increased Promptly and Temporarily after Left Pneumonectomy

Histological appearance showed that there was initially a significant increase in the right lung alveolar duct size in the PNX group in comparison with the THX group. This increase was not so apparent beyond 48 hours (Figure 4A). The calculated alveolar duct area showed a similar trend, showing a significant increase in the PNX groups in comparison with the CON group at 1 hour, followed by a gradual decline over time in the PNX group to a similar level as the CON group (Figure 4B). Statistical significance between CON group and PNX group was lost at 3 days. As for the calculated surface area of the alveoli per volume of lung, in the PNX group it tended to decrease from 1 hour to 24 hours in comparison with the CON group, which was recovered by 48 hours (Figure 4C). The number of alveoli per field also showed a similar trend (Figure 4D), indicating that the decrease in the calculated surface area of the alveoli per volume of lung in the PNX group was primarily due to the increase in the alveolar duct area, and that the sizes of the alveoli were not altered during this period. These results suggested that the immediate increase in LVI was managed primarily through the expansion of the alveolar duct, which was restored, possibly by a subsequent increase in the number of surrounding alveolar septal cells.

Alveolar Septal Cell Proliferation after Left Pneumonectomy Was Most Prominent in the ADS Cells

Further analysis by immunohistochemistry showed that overall, the proportion of alveolar septal cells with Ki-67–positive nuclei was significantly increased beyond 12 hours in the PNX group until 7 days in comparison with the CON group (Figure 5A). The difference was not significant at 14 days. This tendency was similar in AL, AD, and ADS cells, but the magnitude of increase seemed to be most prominent in the ADS cells particularly at 48 hours (Figures 5B–5E). Furthermore, the number of ADS cell nuclei per field increased transiently and significantly at 24 and 48 hours in the PNX group (Figure 6), suggesting that these cells have proliferated and that they may have been incorporated into the newly formed alveolar septal cells.

Transient TTF-1 Knockdown Temporarily Delayed Compensatory Lung Growth

In the PNXsi#2 and PNXsi#4 groups, expression of TTF-1 mRNA was reduced at 12 hours in comparison with the PNXnonsi group (Figure 7A). TTF-1 expression by Western analysis was significantly reduced in comparison with the PNXnonsi group at 48

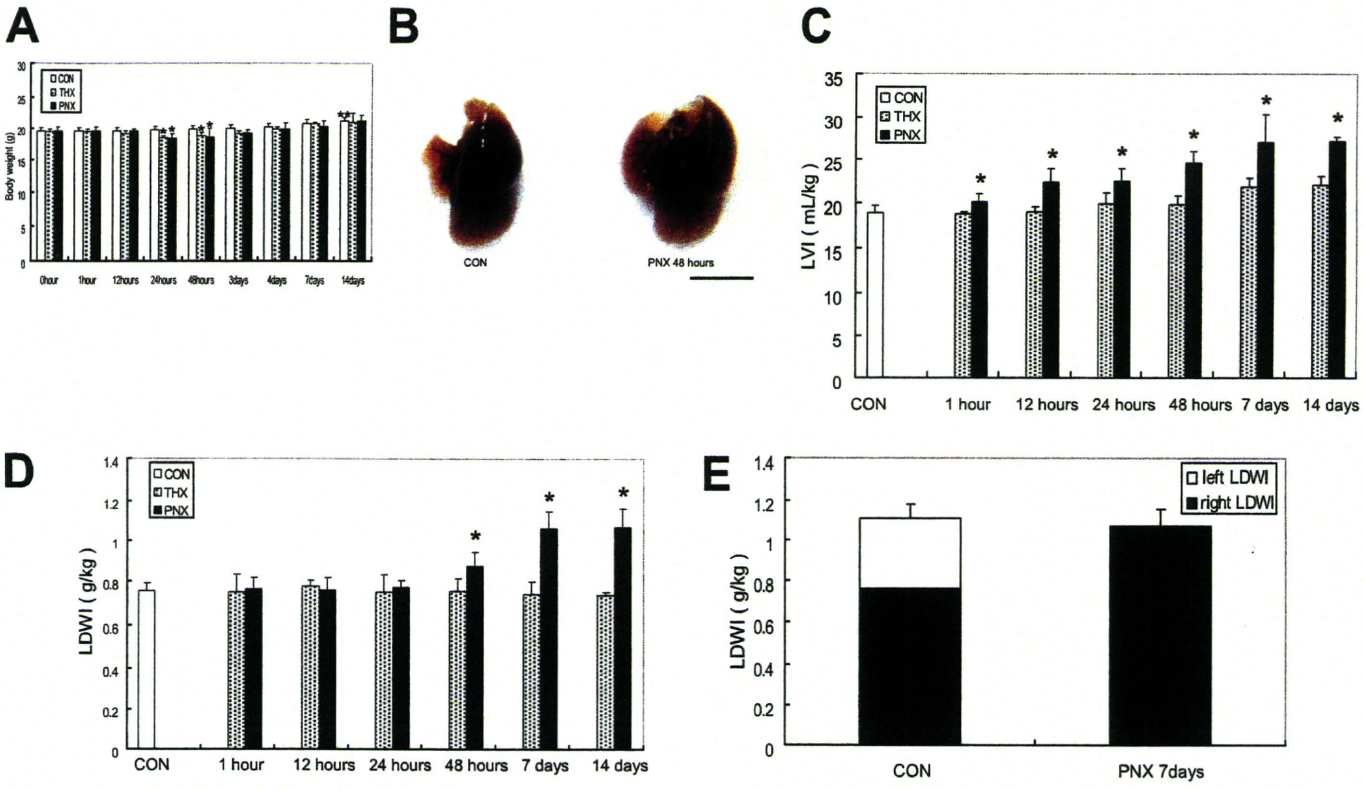

Figure 3. Compensatory lung growth was evaluated in the right lung after left pneumonectomy (PNX group), left thoracotomy (THX group), or no intervention (CON group). (*A*) The body weight of the mice was reduced in the PNX (n = 4) and THX (n = 4) groups in comparison with the CON (n = 4) group at 24 and 48 hours, but was regained from Day 3. The body weight of the mice did not differ significantly between the PNX group and the THX group throughout the observation period; $*P = 0.02$ versus respective CON. In the CON group, body weight was significantly increased at 14 days in comparison with 0, 1, 12, and 24 hours, indicating animal growth, $**P < 0.05$ versus CON group at 0, 1, 12, and 24 hours. (*B*) On gross appearances of the fixed specimens, the residual right lung seemed to be larger in the PNX group in comparison with the CON group at 48 hours (scale bar, 5 mm). (*C*) Lung volume index (LVI) in the right lung increased significantly in the PNX (n = 4 for each time point) group in comparison with the THX (n = 4 for each time point) group beyond 1 hour. Within the PNX group, this increase in LVI continued until 7 days but leveled off at 14 days. There was no significant change within the THX group during this period, and no significant differences between the THX group and the CON (n = 4) group, $*P < 0.05$ versus CON and THX at corresponding time points. (*D*) Lung dry weight index (LDWI) in the right lung did not increase significantly in the PNX (n = 4 for each time point) group in comparison with the THX (n = 4 for each time point) group until 48 hours. Within the PNX group, this increase leveled off beyond 7 days. There were no significant changes in LDWI within the THX group during this period and no significant differences between the THX group and the CON (n = 5) group, $*P < 0.05$ versus CON and THX at corresponding time points. (*E*) LDWI of the right lung in the PNX (n = 4) group at 7 days was not statistically different from the total LDWI (right plus left) in the CON group (n = 5).

hours (Figure 7B). The effect of TTF-1 knockdown was transient, as this difference was not apparent at 7 days (Figure 7C). LDWI was also significantly decreased in the PNXsi#2 and PNXsi#4 groups in comparison with the PNXnonsi group at 48 hours, but was restored to a similar level as the PNXnonsi group by 7 days (Figure 7D). TTF-1 expression was not significantly different between the THXsi#2 and the THXsi#4 group in comparison with the THXnonsi group at 48 hours (Figure 7E). Histological studies showed no apparent indications of lung injury after TTF-1siRNA administration (data not shown). In the PNXsi#2 and PNXsi#4 groups, the alveolar duct area remained significantly increased at 48 hours in comparison with the PNXnonsi group (Figure 7F). This difference was not significant in the THXsi#2, THXsi#4, and THXnonsi groups at 48 hours (Figure 7G), indicating that the increase in alveolar duct area in the right lung after left pneumonectomy was prolonged by TTF-1 knockdown. These results suggested that TTF-1siRNA administration transiently suppressed the induction of TTF-1 in the right lung after left pneumonectomy without significantly affecting the baseline expression of TTF-1. Furthermore, compensatory growth in alveolar septal cells was temporarily delayed as a result of transient TTF-1 knockdown.

DISCUSSION

TTF-1 is a member of the Nkx2 family of homeodomain-containing transcription factors and is selectively expressed in the forebrain, the thyroid, and the lung. TTF-1 is required for lung morphogenesis, and is precisely regulated throughout lung development (20, 21). In the postnatal lung, TTF-1 is expressed primarily in type II epithelial cells and is required for the transcription of surfactant protein–associated genes (22).

In the present study, TTF-1 protein expression in the residual right lung was increased in the PNX group in comparison with the THX group. This increase was most significant in the PNX group at 12 hours, suggesting that TTF-1 may play a role in regulating the early phase of compensatory lung growth. From previous reports in rats, after a rapid phase of overinflation, compensatory lung growth progresses within 4 days followed later by a remodeling phase beyond 2 weeks up to 1 month (23).

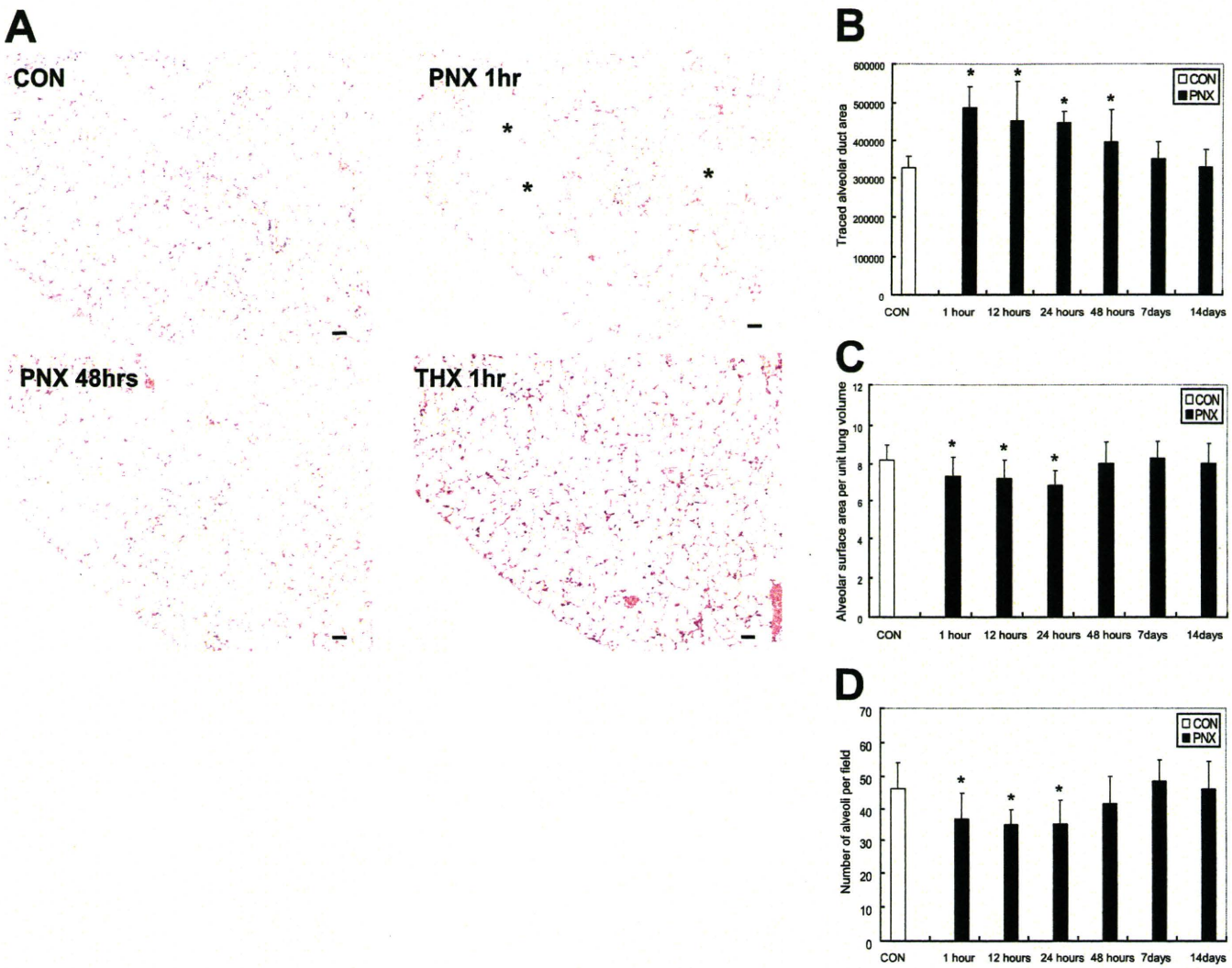

Figure 4. Morphological changes during compensatory lung growth in the right lung after left pneumonectomy (PNX group) or no intervention (CON group). (*A*)There was initially a significant increase in the right lung alveolar duct size in the PNX group (asterisks indicate representative expanded alveolar ducts) in comparison with the THX group. This increase was not so apparent beyond 48 hours (scale bars, 100 μm). (*B*) The alveolar duct area was traced using Image J. Within the PNX group (n = 4, 20 fields for each time point), the calculated alveolar duct area at 1 hour showed a significant increase in comparison with the CON (n = 4, 20 fields) group, followed by a gradual decline over time to a similar level as the CON group. Statistical significance between CON group and PNX group was lost beyond 3 days, $*P < 0.0001$ versus CON. (*C*) The surface area of the alveoli per unit lung volume was calculated as described in the methods. The calculated surface area of the alveoli per unit lung volume in the PNX (n = 4, 20 fields for each time point) group tended to decrease from 1 hour to 24 hours in comparison with the CON (n = 4, 20 fields) group, which was recovered by 48 hours, $*P < 0.03$ versus CON. (*D*) The change in number of alveoli per field in the PNX (n = 4, 20 fields for each time point) group also showed a similar trend in comparison with the CON (n = 4, 20 fields) group as the surface area of the alveoli per unit lung volume, $*P < 0.0001$ versus CON.

But morphological studies looking at the earlier phase of compensatory lung growth are still few. Based on the TTF-1 expression data, we examined the morphological changes focusing primarily on the early phase of compensatory lung growth after left pneumonectomy in mice. In the present study, compensatory lung growth was apparent beyond 48 hours and leveled off at approximately 7 days, as shown by the changes in residual right LDWI. The increase in the residual right LDWI was preceded by the swift increase in the residual right LVI after left pneumonectomy. Morphological analyses showed that the alveolus size did not change significantly during compensatory lung growth, and suggested that the initial increase in lung volume was primarily due to the increase in alveolar duct size, which was evident as early as 1 hour, corresponding with the increase in residual right LVI. The increase in alveolar duct area was alleviated beyond 48 hours presumably due to compensatory growth of the surrounding alveolar septal cells.

It is known that lung distention, or mechanical stretch, has an important role in the initiation of compensatory lung growth and is possibly more influential than hypoxia or changes in pulmonary blood flow (24). The present results suggested that distention was initially most prominent in the right lung alveolar duct region after left pneumonectomy. Analysis of proliferation by regional subgrouping of alveolar septal cells into AL, AD, and ADS cells suggested that initial compensatory lung growth may have occurred primarily through the proliferation of ADS cells, which exist in the vicinity of the extended alveolar duct. Increase in ADS cells may represent septation, possibly from AD cells or the

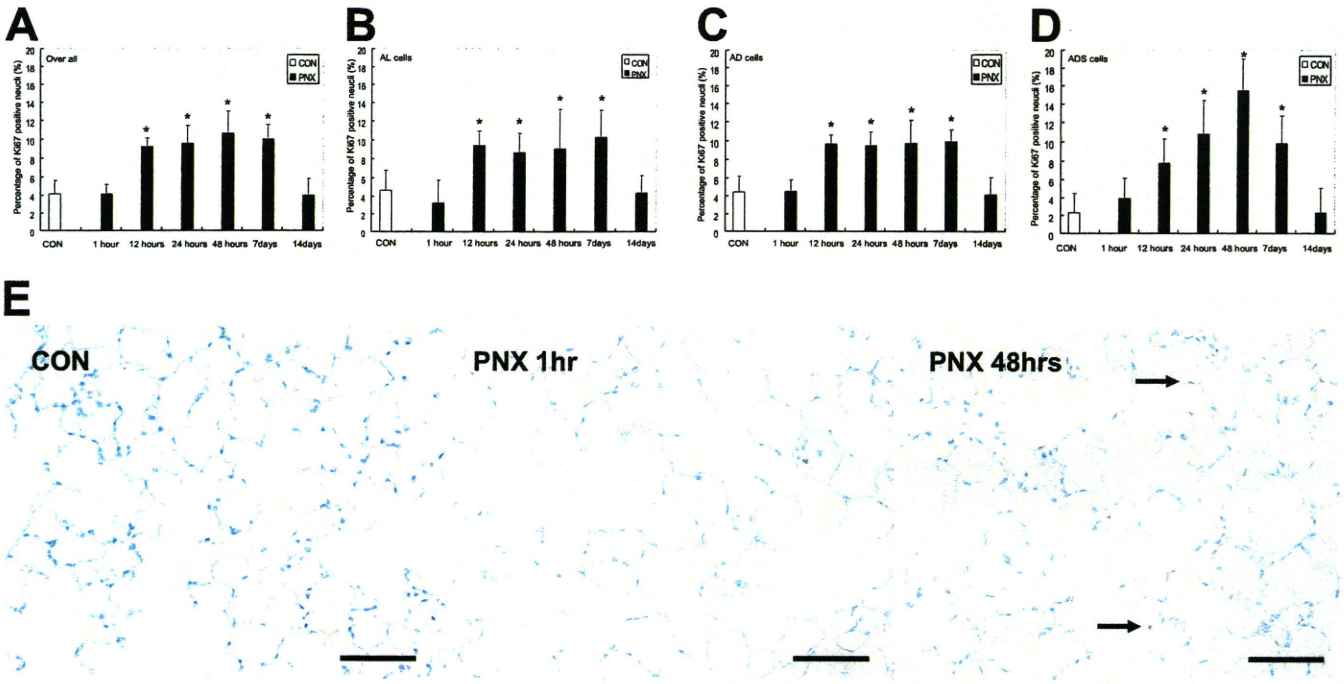

Figure 5. Cell proliferation was evaluated sequentially in the right lung after left pneumonectomy (PNX group), or no intervention (CON group) by Ki-67 immunostaining. (*A*) By immunohistochemistry, the overall proportion of alveolar septal cells with Ki-67–positive nuclei was significantly increased beyond 12 hours in the PNX group (n = 4, 20 fields at each time point) until 7 days in comparison with the CON group (n = 4, 20 fields). The difference was not significant at 14 days, $*P < 0.01$ versus CON, PNX 1 hour, and PNX 14 days. This tendency was similar in (*B*) alveolus (AL) cells, $*P < 0.03$ versus CON, 1 hour, and 14 days; (*C*) alveolar duct (AD) cells, $*P < 0.001$ versus CON, 1 hour, and 14 days; and (*D*) septal structure protruding into the alveolar duct (ADS) cells, $*P < 0.003$ versus CON, 1 hour, and 14 days. (*D* and *E*) The magnitude of increase seemed to be most prominent in the ADS cells, particularly at 48 hours (*arrows* indicate Ki-67–positive ADS cells, scale bars, 100 μm).

cells in the vicinity of the alveolar duct, and at least on qualitative morphology the process appeared to be resembling septation in lung development. Furthermore, preceding the increase in Ki-67–positive cells, the proportion of TTF-1–positive cells was most prominently increased in the AD cells where presumably the magnitude of stretching was greatest. These results suggest that a process resembling septation may have occurred through the proliferation of ADS cells, which was correlated with the increase in TTF-1 expression in the stretched AD cells. The TTF-1–positive cells were also proSPC-positive, indicating that these are type II alveolar cells. Furthermore, transient TTF-1 knockdown temporarily but significantly delayed the alleviation of alveolar duct expansion and compensatory lung growth at 48 hours. The results of this study correlatively suggest that TTF-1 influences the early phase of compensatory lung growth. Compensatory lung growth may be initiated by mechanical stretch in the alveolar duct region leading to a process resembling septation, which presumably occurs at least in part via reactivation of normal developmental pathways. What triggers compensatory lung growth is still not clear, but factors known to be important during normal lung development, such as TTF-1, may be transiently reactivated during the early phase of compensatory lung growth and possibly initiate the process. Lung-specific TTF-1 overexpression after pneumonectomy as well as TTF-1 knockdown may provide additional evidence, but because pneumonectomy by itself significantly elevates TTF-1 expression, the results of such experiments may be difficult to interpret.

Other possibilities remain, such as the transient elevation of TTF-1 in the present study being a part of an injury-repair response (25). However, at least morphologically, we found no apparent indications of lung injury in the residual lung after pneumonectomy. We consider that even if TTF-1 elevation is a repair response, it can still be considered as an important factor in compensatory lung growth, because compensatory lung growth may itself require, at least in part, an injury-repair response. Notwithstanding, the role of TTF-1 in lung development and compensatory lung may need to be distinguished. Recent reports

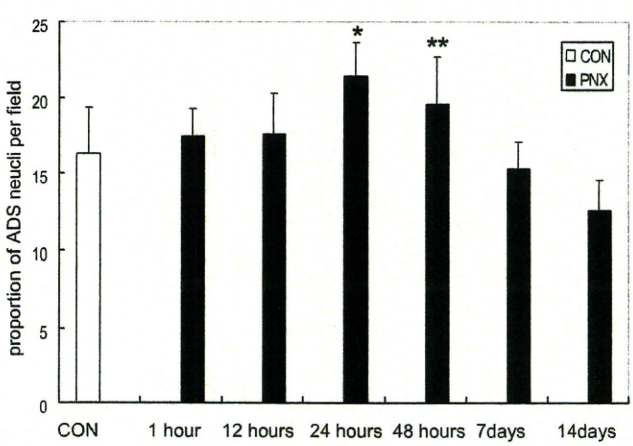

Figure 6. The proportion of the nuclei of the cells in the septal structure protruding into the alveolar duct (ADS) per field was increased transiently but significantly at 24 and 48 hours in the left pneumonectomy (PNX; n = 4, 20 fields for each time point) group; $*P < 0.02$ versus CON group (n = 4, 20 fields) and all other time points; $**P < 0.02$ versus CON group and other time points except PNX 12 hours.

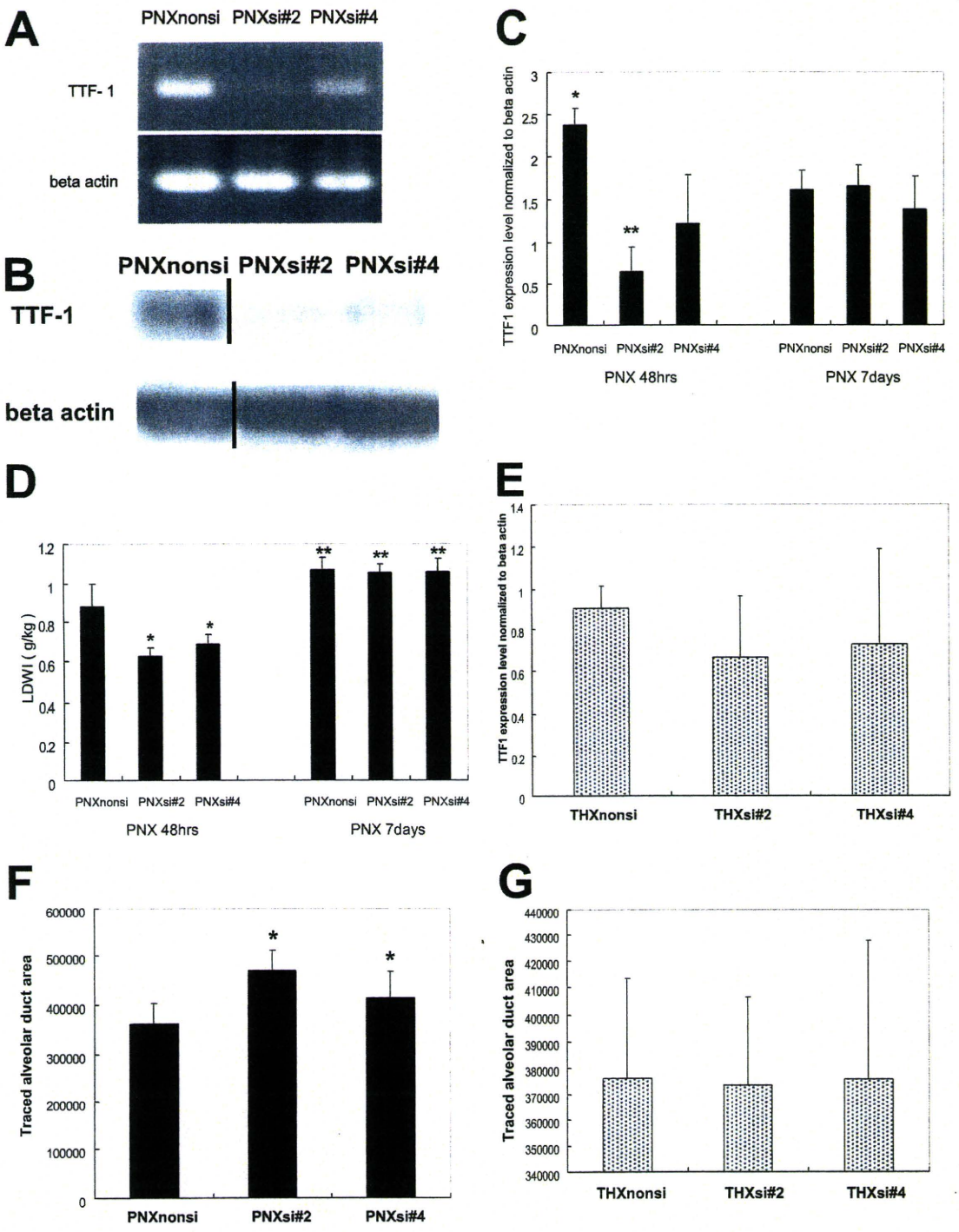

Figure 7. After left pneumonectomy and subsequent intranasal administration of small inhibitory RNAs (siRNAs) (PNXsi#2, PNXsi#4, and PNXnonsi groups) or thoracotomy and subsequent intranasal administration of siRNAs (THXsi#2, THXsi#4, and THXnonsi groups), thyroid transcription factor 1 (TTF-1) expression level in the right lung was measured. Densitometry values were normalized to β-actin for Western blot analyses. (*A*) Mouse TTF-1 mRNA expression was analyzed by reverse transcriptase–polymerase chain reaction at 12 hours. In the PNX group, the TTF-1 mRNA expression level was decreased by the administration of siRNAs. (*B*) In the PNX group, administration of siRNAs significantly reduced TTF-1 expression level at 48 hours. TTF-1 and β-actin for the PNXnonsi group was taken from a separate gel. (C) In the PNXsi#2 (n = 5) and PNXsi#4 (n = 5) groups, TTF-1 expression by Western blot analysis was significantly reduced in comparison with the PNXnonsi (n = 5) group at 48 hours. At 7 days, the level of TTF-1 expression was significantly reduced in all groups in comparison with the PNXnonsi group at 48 hours. The effect of administration of siRNAs was no longer apparent at 7 days. $*P < 0.03$ versus all other measurements; $**P < 0.03$ versus all other measurements except PNXsi#2 at 48 hours. (*D*) Right lung dry weight index (LDWI) was significantly decreased in the PNXsi#2 (n = 4) and PNXsi#4 (n = 4) groups in comparison with the PNXnonsi (n = 4) group 48 hours, but was restored to a similar level as the PNXnonsi (n = 4) group by 7 days, $*P < 0.05$ versus PNXnonsi at 48 hours; $**P < 0.05$ versus all measurements at 48 hours. (*E*) TTF-1 expression was not significantly different between the THXsi#2 (n = 3) and the THXsi#4 (n = 3) group in comparison with the THXnonsi (n = 3) group at 48 hours. (*F*) Alveolar duct area was traced using Image J. In the PNXsi#2 (n = 3), and PNXsi#4 (n = 3) groups, alveolar duct area remained significantly increased at 48 hours in comparison with the PNXnonsi (n = 3) group, $*P < 0.01$ versus PNXnonsi. (*G*) The difference in alveolar duct area was not significant in the THXsi#2 (n = 3), THXsi#4 (n = 3), and THXnonsi (n = 3) groups at 48 hours.

indicate that TTF-1 works in concert with multiple coactivators to achieve normal alveolarization in lung development (26, 27). Observations into the changes in the potential downstream effectors of TTF-1 will be necessary to further dissect the potential mechanisms involved in compensatory lung growth.

In the present study, it is likely that we observed primarily the changes in alveolar cells rather than the endothelial cells or the interstitial cells, which also play important roles in compensatory alveolar septal tissue growth (28). TTF-1 was considered to be expressed predominantly in the type II alveolar cells, but further

studies are necessary to clarify the contribution of individual alveolar septal cell types. We also understand that the definition of AL, AD, and ADS cells is quite subjective. But we consider this to be the limit of light microscopic studies using fixed time point specimens to observe the potential involvement of septation in compensatory lung growth. Techniques such as real-time lung microscopy will be required to further elucidate the sequential events that may be occurring during the early phase of compensatory lung growth. In addition, not only left pneumonectomy but also positive pressure ventilation may have influenced TTF-1 expression, as the protein level was slightly elevated in the THX group in comparison with the CON group, although statistical significance was not reached.

Evolving knowledge in tissue engineering and regeneration may some day accomplish the assembly of functional lung tissue *ex vivo*. But for the meantime, facilitation of compensatory lung growth in the residual lung may be a more attainable goal to improve residual lung function after resection. Certain pharmacological agents have been reported to increase TTF-1 expression in alveolar cells *in vitro* (29). The results of the present study suggest that lung-specific TTF-1 augmentation, possibly through the airway, may be one candidate for therapeutic facilitation and/or reactivation of compensatory lung growth after lung resection in adult humans. It is intuitively understood that compensatory lung growth requires the synchrony and balance of multiple pathways. Manipulation of transcription factors such as TTF-1 may be influential in that it is capable of regulating multiple pathways simultaneously. But because sustained overexpression of TTF-1 has been shown to impair alveolarization in the postnatal lung (25), it is likely that TTF-1 needs to be finely controlled to appropriately orchestrate the early phase of compensatory lung growth. It is also speculated that the lung stem cell population may exist within the AD and/or the ADS cells (30). Although their potential role in compensatory lung growth may be marginal (31), further research is needed in this area.

In this study, the mouse postpneumonectomy lung growth model was used because of its reliability, reproducibility, and establishment as a model of lung growth. To examine the early phase of compensatory lung growth, we used 9-week-old mice because these mice are mature but are still considered to have high plasticity for postnatal lung growth and/or compensatory lung growth. Conversely, it is true that these mice are still in a growth phase as indicated by the increase in body weight during the experiment; hence, the relevance of this model to adult humans may be limited. Nevertheless, we believe that the present model allows us to effectively dissect potentially new mechanisms into the regulation, and possibly induction, of compensatory lung growth. Further studies in aged mice and other animal species may provide more clinically relevant data regarding the potential induction or facilitation of compensatory lung growth after lung resection in adult humans.

Conflict of Interest Statement: None of the authors has a financial relationship with a commercial entity that has an interest in the subject of this manuscript.

Acknowledgment: The authors thank Hitoshi Abe, Department of Pathology, School of Medicine, Keio University, for his expertise in immunohistochemistry. The authors thank Kei Tsujioka, Division of General Thoracic Surgery, School of Medicine, Keio University, for her expertise in animal experiments.

References

1. Laros CD, Westermann CJ. Dilatation, compensatory growth, or both after pneumonectomy during childhood and adolescence. A thirty-year follow-up study. *J Thorac Cardiovasc Surg* 1987;93: 570–576.
2. Nakajima C, Kijimoto C, Yokoyama Y, Miyakawa T, Tsuchiya Y, Kuroda T, Nakano M, Saeki M. Longitudinal follow-up of pulmonary function after lobectomy in childhood-factors affecting lung growth. *Pediatr Surg Int* 1988;13:341–345.
3. Kriesel D, Krupnick AS, Huddleston CB. Outcomes and late complications after pulmonary resections in pediatric population. *Semin Thorac Cardiovasc Surg* 2004;16:215–219.
4. Binns OA, DeLima NF, Buchanan SA, Lopes MB, Cope JT, Marek CA, King RC, Laubach VE, Tribble CG, Kron IL. Mature pulmonary lobar transplants grow in an immature environment. *J Thorac Cardiovasc Surg* 1997;114:186–194.
5. Fehrenbach H, Voswinckel R, Michl V, Mehling T, Fehrenbach A, Seeger W, Nyengaard JR. Neoalveolarisation contributes to compensatory lung growth following pneumonectomy in mice. *Eur Respir J* 2008;31:483–485.
6. Voswinckel R, Motejl V, Fehrenbach A, Wegmann M, Mehling T, Fehrenbach H, Seeger W. Characterisation of post-pneumonectomy lung growth in adult mice. *Eur Respir J* 2004;24:524–532.
7. Kaza AK, Laubach VE, Kern JA, Long SM, Fiser SM, Tepper JA, Nguyen RP, Shockey KS, Tribble CG, Kron IL. Epidermal growth factor augments postpneumonectomy lung growth. *J Thorac Cardiovasc Surg* 2000;120:916–921.
8. Sakamaki Y, Matsumoto K, Mizuno S, Miyoshi S, Matsuda H, Nakamura T. Hepatocyte growth factor stimulates proliferation of respiratory epithelial cells during postpneumonectomy compensatory lung growth in mice. *Am J Respir Cell Mol Biol* 2002;26:525–533.
9. Kaza AK, Kron IL, Leuwerke SM, Tribble CG, Laubach VE. Keratinocyte growth factor enhances post-pneumonectomy lung growth by alveolar proliferation. *Circulation* 2002;24:I120–I124.
10. Sakurai MK, Lee S, Arsenault DA, Nose V, Wilson JM, Heymach JV, Puder M. Vascular endothelial growth factor accelerates compensatory lung growth after unilateral pneumonectomy. *Am J Physiol Lung Cell Mol Physiol* 2007;292:L742–L747.
11. Mason RJ. Hepatocyte growth factor: the key to alveolar septation? *Am J Respir Cell Mol Biol* 2002;26:517–520.
12. Stahlman MT, Gray ME, Whitsett JA. Expression of thyroid transcription factor-1(TTF-1) in fetal and neonatal human lung. *J Histochem Cytochem* 1996;44:673–678.
13. Yang MC, Guo Y, Liu CC, Weissler JC, Yang YS. The TTF-1/TAP26 complex differentially modulates surfactant protein-B (SP-B) and -C (SP-C) promoters in lung cells. *Biochem Biophys Res Commun* 2006; 344:484–490.
14. Scherle W. A sample method for volumetry of organs in quantitative stereology. *Mikroskopie* 1970;26:57–60.
15. Weibel ER. Stereological methods. In: E. R. Weiber, ed. Practical methods for biological morphometry. London: Academic Press; 1979.
16. Kawakami M, Paul JL, Thurlbeck WM. The effect of age on lung structure in male BALB/cNNia inbred mice. *Am J Anat* 1984;170:1–21.
17. Inselman LS, Pedilla-Burgos LB, Teichberg S, Spencer H. Alveolar enlargement in obesity-induced hyperplastic lung growth. *J Appl Physiol* 1988;65:2291–2296.
18. Massaro D, Massaro GD, Clerch LB. Noninvasive delivery of small inhibitory RNA and other reagents to pulmonary alveoli in mice. *Am J Physiol Lung Cell Mol Physiol* 2004;287:L1066–L1070.
19. Li C, Cai J, Pan Q, Minoo P. Two functionally distinct forms of Nkx2.1 protein are expressed in pulmonary epithelium. *Biochem Biophys Res Commun* 2000;270:462–468.
20. Kimura S. Thyroid-specific enhancer-binding protein role in thyroid function and organogenesis. *Trends Endocrinol Metab* 1996;7:247–252.
21. Minoo P, Su G, Drum H, Bringas P, Kimura S. Defects in tracheoesophageal and lung morphogenesis in Nkx2.1(−/−) mouse embryos. *Dev Biol* 1999;209:60–71.
22. Kelly SE, Bachurski CJ, Baurhans MS, Glasser SW. Transcription of the lung-specific surfactant protein C gene is mediated by thyroid transcription factor 1. *J Biol Chem* 1996;271:6881–6888.
23. Berger LC, Burri PH. Timing of the quantitative recovery in the regenerating rat lung. *Am Rev Respir Dis* 1985;132:777–783.
24. Brown LM, Rannels SR, Rannels DE. Implications of post-pneumonec tomy lung growth in pulmonary physiology and disease. *Respir Res* 2001;2:340–347.
25. Wert SE, Dey CR, Blair PA, Kimura S, Whitsett JA. Increased expression of thyroid transcription factor-1 (TTF-1) in respiratory epithelial cells inhibits alveolarization and causes pulmonary inflammation. *Dev Biol* 2002;242:75–87.
26. Mitani A, Nagase T, Fukuchi K, Aburatani H, Makita R, Kurihara H. Transcriptional coactivator with PDZ-binding motif is essential for

normal alveolarization in mice. *Am J Respir Crit Care Med* 2009;180: 326–338.
27. Kurotani R, Tomita T, Yang Q, Carlson BA, Chen C, Kimura S. Role of secretoglobin 3A2 in lung development. *Am J Respir Crit Care Med* 2008;178:389–398.
28. Hsia CC, Johnson RL Jr. Further examination of alveolar septal adaptation to left pneumonectomy in the adult lung. *Respir Physiol Neurobiol* 2006;151:167–177.
29. Kolla V, Gonzales LW, Gonzales J, Wang P, Angampalli S, Feinstein SI, Ballard PL. Thyroid transcription factor in differentiating type II cells: regulation, isoforms, and target genes. *Am J Respir Cell Mol Biol* 2006;36:213–225.
30. Giangreco A, Reynolds SD, Stripp BR. Terminal bronchioles harbor a unique airway stem cell population that localizes to the bronchoalveolar duct junction. *Am J Pathol* 2002;161:173–182.
31. Nolen-Walston RD, Kim CF, Mazan MR, Ingenito EP, Gruntman AM, Tsai L, Boston R, Woolfenden AE, Jacks T, Hoffman AM. Cellular kinetics and modeling of bronchioalveolar stem cell response during lung regeneration. *Am J Physiol Lung Cell Mol Physiol* 2008;294: L1158–L1165.

Jpn J Clin Oncol 2010;40(10)986–988
doi:10.1093/jjco/hyq067
Advance Access Publication 21 May 2010

Case Reports

A Non-invasive Thymoma that Occurred 29 Years After Complete Resection of a Non-invasive Thymoma Accompanied by a Microthymoma

Yoshikane Yamauchi[1,*], Mitsutomo Kohno[1], Tai Hato[1], Yuichiro Hayashi[2], Yotaro Izumi[1] and Hiroaki Nomori[1]

[1]Department of Surgery, School of Medicine, Keio University and [2]Department of Pathology, School of Medicine, Keio University, Tokyo, Japan

*For reprints and all correspondence: Yoshikane Yamauchi, Department of Surgery, School of Medicine, Keio University, 35 Shinanomachi, Shinjuku-ku, Tokyo 160-8582, Japan. E-mail: yoshikaney@2004.jukuin.keio.ac.jp

Received October 11, 2009; accepted April 10, 2010

A 55-year-old woman with a 7 cm non-invasive thymoma and myasthenia gravis had been treated by extended thymectomy via median sternotomy 29 years ago. A microscopic 0.15 cm thymoma (microthymoma) was incidentally found in the thymus during surgery. Twenty-nine years later, a 5 cm thymoma developed in the anterior mediastinum and was surgically treated. The non-invasive first thymoma, the microthymoma and the non-invasive third thymoma were all classified as type AB thymomas according to the World Health Organization (WHO) classification and showed extremely similar histological findings. We think the mechanism underlying the local recurrence of non-invasive thymomas would be intrathymic metastasis because of their clinical and pathological features.

Key words: thymoma – local recurrence – multicentric development – intrathymic metastasis – microthymoma

INTRODUCTION

Thymoma is a low-grade malignant tumor generally associated with a good prognosis after surgical treatment. However, in the case of non-invasive thymomas, there is a 1.3–5.4% chance of local recurrence even after complete resection (1–3). Local recurrence after complete resection of non-invasive thymomas has been reported to be caused by multicentric development of thymomas (1). In 1990, we reported the case of a 26-year-old woman with two synchronous thymomas: (i) a non-invasive thymoma that was 7 cm in size and (ii) a microscopic thymoma (microthymoma) that was 0.15 cm in size (4). Twenty-nine years later, the patient developed another thymoma, which was again treated by surgical resection. Here, we discuss the mechanism underlying the development of these 3 thymomas by comparing their histological findings.

CASE REPORT

The patient was a 55-year-old woman. At the age of 26 years, she had undergone extended thymectomy via median sternotomy for a non-invasive thymoma and generalized myasthenia gravis (MG). The thymoma was 7 cm in size; a 0.15 cm well-encapsulated microthymoma was incidentally found in the thymus. The histological features of the microthymoma were quite similar to those of the larger tumor, which was reported by one of our coauthors (H.N.) in 1990 (4). Because the symptoms of MG diminished soon after surgery, she decided to stop visiting us.

In October 2008, 29 years after the initial treatment, she complained of general fatigue again. Chest computed tomography revealed an anterior mediastinal mass 5 cm in size (Fig. 1). Although the result of the tensilon test was negative, the serum anti-acetylcholine receptor antibody (anti-achR Ab) level was elevated to 41 nmol/l. In December 2008, the tumor was resected via left thoracotomy. The tumor was located at the anterolateral side of the aortic arch, anterior to the phrenic nerve and adjacent to the sternum, pericardium and upper lobe of the left lung. The tumor was resected concomitant with wedge resection of the upper lobe of the left lung (Fig. 2). Pathological examination revealed a fibrous thick wall totally covering the tumor; the diagnosis was a

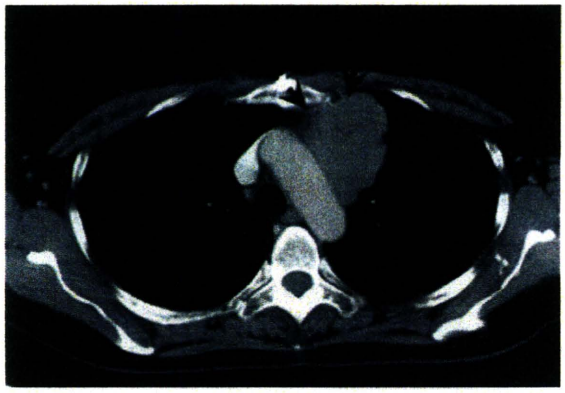

Figure 1. Computed tomography performed 29 years after the first surgery, showing a well-defined mass in the anterior mediastinum, adjacent to the aortic arch. The arrows indicate the margin of the tumor.

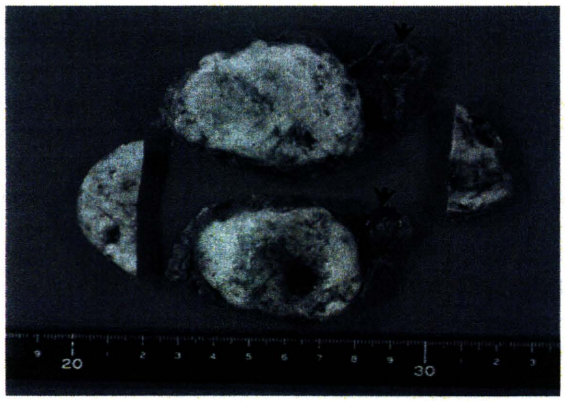

Figure 2. Anterior mediastinal tumor resected in the second surgery, in which wedge resection of the upper lobe of the left lung (arrow) was also performed.

non-invasive thymoma of histological type AB. Capsular invasion was not observed microscopically or macroscopically. The histological features of the tumor were quite similar to those of the two thymomas that were detected 29 years ago (Fig. 3).

Although her post-operative clinical course was fair, her general fatigue did not improve because of the elevation of the serum level of anti-achR Ab up to 170 nmol/l. Her condition was not symptomatic enough for MG to be diagnosed, but the induction of pyridostigmine bromide therapy significantly improved her symptoms. To date (i.e. 1 year after the second surgery), she has remained healthy and asymptomatic and is on oral pyridostigmine bromide therapy.

DISCUSSION

The recurrence rate of non-invasive thymomas after resection has been reported to be 1.3–5.4% (1–3); the tumor sometimes recurs many years after complete resection because of its slow growth rate. Awad et al. (4) reported a case of local recurrence of non-invasive thymoma 37 years after complete resection of the tumor. Nomori et al. (5) reported a case in which non-invasive thymoma developed over 20 years before it was detected; the patient developed pulmonary metastases 12 years after it had been resected, resulting in a 32-year clinical course.

The mechanism underlying the local recurrence of non-invasive thymomas is controversial, but the following mechanisms have been posited: (i) local recurrence at the surgical margin; (ii) lymph node metastasis; (iii) multicentric development of thymomas in the remnant thymic tissue; and (iv) intrathymic metastasis in the remnant thymic tissue. Because all the thymomas in this patient were non-invasive, the possibility of local recurrence at the surgical margin can be

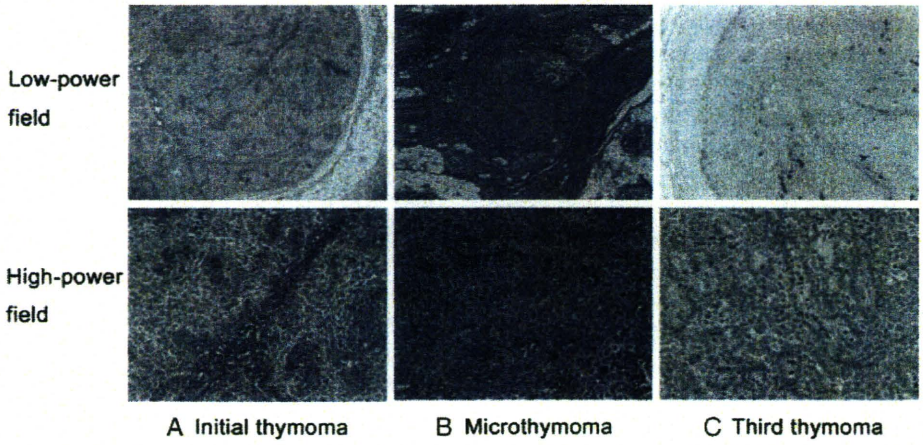

Figure 3. Comparison of the histological findings of the specimens obtained from the two surgeries. (a) Non-invasive thymoma obtained during the initial resection. (b) Microthymoma obtained during the initial resection. (c) Non-invasive thymoma obtained during the second resection. The tumors were solid and consisted of thymic epithelial cells with abundant cytoplasm, round-to-oval-shaped vesicular nuclei and inconspicuous nucleoli with a strand-like pseudoglandular structure (low-power field: H&E, ×10; high-power field: H&E, ×100). A few lymphocytes are scattered among the epithelial cells. The histological findings were very similar for the three tumors.

excluded, although it is hard to determine whether multicentric development or the intrathymic metastasis caused the development of multiple thymomas. We could not exclude the possibility that the third thymoma occurred because of lymph node metastasis. However, thymomas rarely metastasize to the lymph nodes, and lymph node metastasis has not occurred in this patient to date. Moreover, the recurrent tumor did not exhibit any histological structures characteristic of lymph node tissue. Therefore, the third tumor may not be a lymph node metastasis. Mori et al. (6) reviewed the histological types of thymomas in 12 patients with multiple thymomas, including 3 of their own patients, and reported that 10 patients (83%) had the same histological subtypes. Although they concluded that most multiple thymomas might develop from identical tumorigenesis, we prefer the hypothesis that intrathymic metastasis caused the development of multiple thymomas in the present case for the following reasons: (i) all the thymomas exhibited extremely similar histological features; (ii) the sizes of the two thymomas detected initially were significantly different (i.e. 7 cm and 0.15 cm), suggesting the possibility that the smaller tumor was an intrathymic metastasis; and (iii) it is quite likely that the third thymoma originated from the intrathymic microscopic metastasis and grew gradually over 29 years because thymomas are characterized by slow growth (4–5). Even though this patient initially underwent extended thymectomy, microscopic thymic tissue could have remained because the distribution of thymic tissue is extensive and complicated (7–8).

Another important issue in the present case is the occurrence of the microthymoma, which was found incidentally in the thymus 29 years ago. The term 'microthymoma' was first proposed for microscopic thymomas by Cheuk et al. (9) in 2005. Mori et al. (10) reviewed seven patients with microthymomas, including three of their own patients and the present case when it was initially reported in 1990. Those microthymomas ranged from 0.15 to 0.7 cm in size, with our patient's microthymoma being the smallest one. The findings for our patient suggest that the occurrence of microthymomas is a risk factor for the recurrence of non-invasive thymomas.

In our patient, because the third tumor was located anterior to the phrenic nerve, it is possible that it might have developed from remnant thymic tissue after the first surgery, even though an extended thymectomy had been performed. Surgeons must exercise great caution to not leave any remnants of thymic tissue while performing extended thymectomy; not to mention that mere extirpation of the tumor is inadequate in the case of thymomas, even if the tumor is encapsulated.

Therefore, while treating thymomas, it is very important not only to perform a 'complete' extended thymectomy but also to perform pathological tests on thin slices of thymic tissue for detecting microthymomas. For patients with microthymoma, a lengthy follow-up (more than 20 years) is essential to determine a local recurrence.

Conflict of interest statement

None declared.

References

1. Bernatz PE, Harrison EG, Clagett OT. Thymoma: a clinicopathologic study. *J Thorac Cardiovasc Surg* 1961;42:424–44.
2. Masaoka A, Monden Y, Nakahara K, Tanioka T. Follow-up study of thymomas with special reference to their clinical stages. *Cancer* 1981;48:2485–92.
3. Strobel P, Bauer A, Puppe B, Kraushaar T, Krein A, Toyka K, et al. Tumor recurrence and survival in patients treated for thymomas and thymic squamous cell carcinomas: a retrospective analysis. *J Clin Oncol* 2004;22:1501–9.
4. Awad WI, Symmans PJ, Dussek JE. Recurrence of stage I thymoma 32 years after total excision. *Ann Thorac Surg* 1998;66:2106–8.
5. Nomori H, Kobayashi K, Ishihara T, Suito T, Torikata C. A case of multiple thymoma: the possibility of intra-thymic metastasis. *Jpn J Clin Oncol* 1990;20:209–11.
6. Mori T, Nomori H, Ikeda K, Yoshioka M, Kobayashi H, Iwatani K, et al. Three cases of multiple thymoma with a review of the literature. *Jpn J Clin Oncol* 2007;37:146–9.
7. Jaretzki A, 3rd, Wolff M. 'Maximal' thymectomy for myasthenia gravis. Surgical anatomy and operative technique. *J Thorac Cardiovasc Surg* 1988;96:711–6.
8. Masaoka A, Yamakawa Y, Niwa H, Fukai I, Kondo S, Kobayashi M, et al. Extended thymectomy for myasthenia gravis patients: a 20-year review. *Ann Thorac Surg* 1996;62:853–9.
9. Cheuk W, Tsang WY, Chan JK. Microthymoma: definition of the entity and distinction from nodular hyperplasia of the thymic epithelium (so-called microscopic thymoma). *Am J Surg Pathol* 2005;29:415–9.
10. Mori T, Nomori H, Ikeda K, Kobayashi H, Iwatani K, Yoshioka M, et al. Microscopic-sized 'microthymoma' in patients with myasthenia gravis. *Chest* 2007;131:847–9.

References

1. Beghetti M, Gow RM, Haney I, et al. Pediatric primary benign cardiac tumors: a 15-year review. Am Heart J 1997;134:1107–14.
2. Burke AP, Rosado-de-Christenson M, Templeton PA, et al. Cardiac fibroma: clinicopathologic correlates and surgical treatment. J Thorac Cardiovasc Surg 1994;108:862–70.
3. Valente M, Cocco P, Thiene G, et al. Cardiac fibroma and heart transplantation. J Thorac Cardiovasc Surg 1993;106: 1208–12.
4. Meissner C, Minnasch P, Gafumbegete E, et al. Sudden unexpected infant death due to fibroma of the heart. J Forensic Sci 2000;45:731–3.
5. Stiller B, Hetzer R, Meyer R, et al. Primary cardiac tumors: when is surgery necessary? Eur J Cardiothorac Surg 2001;20: 1002–6.
6. Bapat VN, Varma GG, Hardikar AA, et al. Right ventricular fibroma presenting as tricuspid stenosis—case report. Thorac Cardiovasc Surg 1996;44:152–4.

Mediastinal Germ Cell Tumor With Somatic-Type Malignancy: Report of 5 Stage I/II Cases

Keisuke Asakura, MD, Yotaro Izumi, MD, PhD, Tatsuhiko Ikeda, MD, Yoshishige Kimura, MD, Hirohisa Horinouchi, MD, PhD, Yuichiro Hayashi, MD, and Hiroaki Nomori, MD, PhD

Division of General Thoracic Surgery, and Department of Pathology, School of Medicine, Keio University, Tokyo, Japan

Among 15 patients with primary mediastinal nonseminomatous germ cell tumors experienced during the past 12 years, 5 were diagnosed with germ cell tumors with somatic-type malignancy. The pretreatment stages were stage I in 2 patients and stage II in 3. All 5 patients received perioperative chemotherapy plus surgical resection, and 4 remain alive without relapse, with a mean follow-up of 60 months.

(Ann Thorac Surg 2010;90:1014–6)

A germ cell tumor with somatic-type malignancy (GCT-STM) is a germ cell tumor (GCT) accompanied by somatic-type malignant (STM) components, such as sarcoma, carcinoma, or both, according to the most recent histologic classification of the World Health Organization [1]. The GCT-STM reportedly accounts for 11% to 29% of all cases of mediastinal GCT in adults [2–4] and is mostly diagnosed from resected specimens. There have also been reports made that patients who have GCT-STM are generally diagnosed at an advanced stage and are resistant to chemotherapy with poor prognoses (mean survival time, 14 to 15 months) [2–6]. An extended case report on stage I-II GCT-STM patients is rare.

Accepted for publication Dec 30, 2009.

Address correspondence to Dr Izumi, Division of General Thoracic Surgery, Department of Surgery, School of Medicine, Keio University, 35 Shinanomachi, Shinjuku-ku, Tokyo, 160-8582, Japan; e-mail: yotaroizumi@a2.keio.jp.

Fifteen patients with mediastinal nonseminomatous GCT were treated with chemotherapy or radiotherapy, or both, plus surgical treatment in Keio University Hospital between 1995 and 2007. Of these, 15 patients, 5 were histologically diagnosed as GCT-STM from the resected specimens. Diagnoses of GCT-STMs were made according to morphologic criteria previously described, and STM components that lacked expansible and invasive growth patterns, which were excluded from the GCT-STM diagnoses [6]. Clinical staging was based on Moran and Suster's [2] staging scheme.

Table 1 summarizes the clinicopathologic features of the 5 patients. The serum α-fetoprotein levels were elevated in all 5 patients before initial treatment. All patients, except patient 1, had undergone chemotherapy before surgery, complemented by a bleomycin, etoposide, cisplatin (BEP) regimen of two to four courses. Patient 1 had first undergone surgical resection at another institution. No STM component was found in the resected specimen. The BEP regimen was done after surgery. Patient 1 presented with local recurrence without serum α-fetoprotein elevation at 7 months after the initial resection; the patient was referred to our institution. Radiologic responses to BEP therapy were progressive disease in patient 1 and no change in the other 4 patients. Serum α-fetoprotein levels decreased to a normal range (0 to 20 ng/mL) in all patients. All 5 patients were treated by complete resection (re-resection in patient 1). The resected specimens showed variable STM components, such as angiosarcoma, glioma, leiomyosarcoma, rhabdomyosarcoma, liposarcoma, osteosarcoma, chondrosarcoma, malignant fibrous histiocytoma, and adenocarcinoma (Table 1, Fig 1). Patient 1 underwent radiation therapy (50 Gy) after re-resection. Patients 2 and 4 had undergone postoperative chemotherapy, with one and three courses, respectively, of a BEP regimen. Of the 5 patients, 4 are alive and without recurrence, between 27 and 132 months after initial treatment. Patient 5 died of disease 19 months after treatment. A needle biopsy for multiple liver metastases in this patient showed metastasis of leiomyosarcoma.

Comment

It has been reported that it is very difficult to diagnose GCT-STM from biopsy specimens, and that such a diagnosis can only be made from resected specimens, typically after chemotherapy [4, 5, 7, 8]. Although Athanasiou and colleagues [8] retrospectively reported that computed tomographic or magnetic resonance imaging findings, or both, in 6 of 14 patients with GCT-STM could indicate the presence of STM components, those findings were of particular types of STM components, such as osteosarcoma showing expanded ossification, adenocarcinoma showing cancerous peritonitis, or bronchioloalveolar carcinoma showing an expanded pulmonary ground-glass opacity-like appearance. However, other STM components would not be easily detected on either computed tomographic or magnetic resonance imaging.

From our present series of patients, we speculate that one characteristic clinical finding of GCT-STM may be a minimal reduction or even an increase in tumor size after

Published by Elsevier Inc
0003-4975/$36.00
doi:10.1016/j.athoracsur.2009.12.081

Table 1. Clinicopathologic Features of 5 Germ Cell Tumor Somatic Type Malignancy Cases

		Final Histology			Tumor Size (cm)		α-Fetoprotein (ng/mL)		
Patient No.	Age/Sex	GCT STM	Stage	BEP	Before	After	Before	After	Outcome
1	24/M	MT AC	II	3	0[a]	6	3	3	Alive: 132 months
2	21/M	IT, YT RMS	I	3	6	5	304	5	Alive: 89 months
3	35/M	MT AS, GL OS, CS, LS	I	2	13		197	6	Alive: 36 months
4	34/M	IT MFH, US	II	2	7	8	377	2	Alive: 27 months
5	45/M	MT GB, LMS, AC	II	4	15	15	27,600	11	Dead: 19 months

[a] Primary resection was done prior to initial chemotherapy.

After = after initial chemotherapy; AC = adenocarcinoma; AS = angiosarcoma; Before = before initial chemotherapy; BEP = courses of bleomycin, etoposide, cisplatin regimen; CS = chondrosarcoma; GB = glioblastoma; GCT = germ cell tumor; GL = glioma; IT = immature teratoma; LMS = leiomyosarcoma; LS = liposarcoma; M = male; MFH = malignant fibrous histiocytoma; MT = mature teratoma; OS = osterosarcoma; RMS = rhabdomyosarcoma; STM = somatic type malignancy; US = unclassified sarcoma; YT = yolk sac tumor.

chemotherapy, despite a normalization of tumor markers. During the same period as the present series, 10 patients presented with primary mediastinal nonseminomatous GCT without STM components. Tumor markers were normalized in 8 of 9 patients who received chemotherapy before resection. Radiologic responses in these 8 patients were complete response in 1, partial response in 3, and no change in 4. In the present series, discrepancies between serum tumor marker response and radiologic response seem to be more common among GCT-STM patients.

There was no STM component in the primary resected specimen of patient 1. The GCT-STM was diagnosed from the re-resected specimen at relapse after chemotherapy. Therefore, it can be speculated that postoperative chemotherapy may have induced the formation of STM component in patient 1. The majority of reports, including our case series, suggest that chemotherapy or radiotherapy may induce the formation of STM component from the malignant transformation of pre-existing teratoma or the induction of differentiation among the pluripotent germ cell components [6, 8], or both. However, no conclusions can be drawn because primary tumor resection is not usually done in this group of patients.

The GCT-STM has been reported to be generally advanced at diagnosis [8], highly metastatic [5], resistant to standard cisplatin-based chemotherapy [5–7], and associated with poorer prognosis than GCT without STM (the reported mean survival time, 14 to 15 months) [2–6]. In our present series of 5 patients with stage I-II GCT-STM, the mean survival time was 60 months. During the same period, 10 patients with primary mediastinal nonseminomatous GCT without STM components underwent surgical

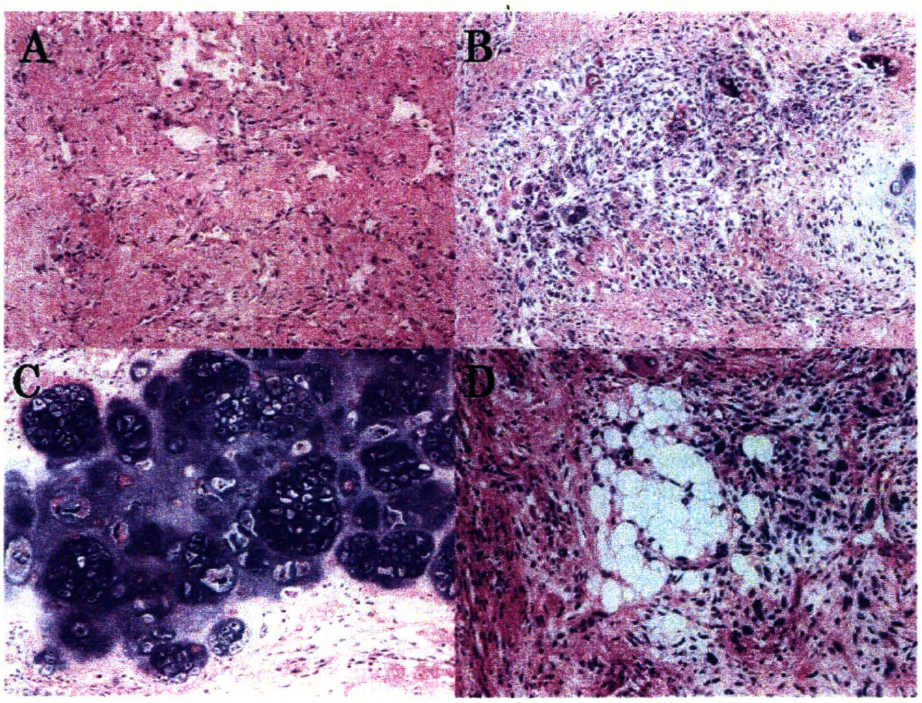

Fig 1. Germ cell tumor with somatic-type malignancy (patient 3). (A) Angiosarcoma component. (Hematoxylin and eosin, ×400.) (B) Osteosarcoma component. (Hematoxylin and eosin, ×400.) (C) Chondrosarcoma component. (Hematoxylin and eosin, ×400.) (D) Liposarcoma component. (Hematoxylin and eosin, ×400.)

Ann Thorac Surg
2010;90:1016–7

resection with perioperative BEP therapy at our institution. Their clinical stages were stage I in 2 patients, stage II in 5, and stage III in 3. The mean survival time of the 7 patients with stage I-II GCT without STM was 84 months, which was not statistically different in comparison with the 5 cases of stage I-II GCT-STM ($p = 0.85$). Prognosis in our 5 patients with GCT-STM was better than previously reported [2–6]. Although most reports do not show the information on clinical stages, Malagon and colleagues [5] reported that clinical stages among 23 patients with mediastinal GCT-STM were stage II in 3 patients, stage III in 15, and unknown in 5. We believe that the specific prognosis of stage I-II mediastinal GCT-STM has not been reported; however, the prognosis may be comparable with stage I-II GCT without STM.

References

1. Travis WD, Muller-Hermelink HK, Harris CC. World Health Organization classification of tumors, pathology and genetics of tumors of the lung, pleura, thymus and heart, 1st ed. Lyon, France: IARC Press; 2004.
2. Moran CA, Suster S. Primary germ cell tumors of the mediastinum: I. Analysis of 322 cases with special emphasis on teratomatous lesions and a proposal for histopathologic classification and clinical staging. Cancer 1997;80:681–90.
3. Wright CD, Kesler KA, Nichols CR, et al. Primary mediastinal nonseminomatous germ cell tumors. Results of a multimodality approach. J Thorac Cardiovasc Surg 1990;99:210–7.
4. Gonzalez-Vela JL, Savage PD, Manivel JC, Torkelson JL, Kennedy BJ. Poor prognosis of mediastinal germ cell cancers containing sarcomatous components. Cancer 1990;66:1114–6.
5. Malagon HD, Valdez AM, Moran CA, Suster S. Germ cell tumors with sarcomatous components: a clinicopathologic and immunohistochemical study of 46 cases. Am J Surg Pathol 2007;31:1356–62.
6. Ulbright TM, Loehrer PJ, Roth LM, Einhorn LH, Williams SD, Clark SA. The development of non-germ cell malignancies within germ cell tumors. A clinicopathologic study of 11 cases. Cancer 1984;54:1824–33.
7. Donadio AC, Motzer RJ, Bajorin DF, et al. Chemotherapy for teratoma with malignant transformation. J Clin Oncol 2003; 21:4285–91.
8. Athanasiou A, Vanel D, El Mesbahi O, Theodore C, Fizaki K. Non-germ cell tumours arising in germ cell tumours (teratoma with malignant transformation) in men: CT and MR findings. Eur J Radiol 2009;69:230–5.

FEATURE ARTICLES

Extraskeletal Ewing's Sarcoma Presenting as a Mediastinal Mass

Jane Halliday, MB BChir,
Sing Yang Soon, MB ChB, MRCS,
Hannah Monaghan, MB BS,
William S. Walker, MB BChir, FRCS, and
Vipin Zamvar, MBBS, FRCS

Department of Cardiothoracic Surgery, Royal Infirmary of Edinburgh, Edinburgh, United Kingdom

Ewing's sarcoma family of tumors is part of a rare group of malignant neoplasms with small blue, round-cell morphology on hematoxylin and eosin stain, expressing CD99, C-Kit, and Bcl2, and sharing the presence of the translocation t(11:22). Extraskeletal Ewing's sarcoma is a rare disease that typically involves the soft tissues of the trunk or extremities. We describe a case of extraskeletal Ewing's sarcoma presenting as a mediastinal mass in a 16-year-old boy.

(Ann Thorac Surg 2010;90:1016–7)

The Ewing's family of tumors are a group of nonhereditary small, blue, round-cell tumors occurring in bone and soft tissues, characterized as a group by the presence of the translocation t(11; 22) (q24; q12). They typically occur in children and young adults, and the majority are osseous in origin. Extraskeletal Ewing's sarcoma is a soft-tissue primary tumor that typically presents as a painful rapidly growing tumor in the lower limb and paravertebral regions.

A 16-year-old boy presented with a 2-day history of dyspnea and stridor at rest. Prior to this acute deterioration he admitted to 6 months intermittent dysphonia and 3 months progressive dyspnea on exertion. He had no other symptoms. On examination he had marked stridor, no lymphadenopathy, and no superior vena cava obstruction. His peak expiratory flow rate was 180 L/min. A right vocal cord palsy was noted during a flexible endoscopy. A chest roentgenogram and computed tomographic scan demonstrated a large upper mediastinal mass with tracheal compression to 5 mm (Fig 1). Thyroid function tests, lactate dehydrogenase, and tumor markers (α-fetoprotein and β-human chorionic gonadotrophin) were normal. An attempted biopsy through a right neck dissection was inconclusive due to sampling error. We elected to perform a right thoracotomy to resect the tumor. Double lumen endotracheal intubation was uneventful. At thoracotomy, we found a large mass in the right paratracheal region. The mass extended from the superior edge of the azygos vein to the thoracic inlet superiorly. Anteroposteriorly it covered the entire apical thoracic cavity. The pleura over the mass were incised. The mass was covered with a capsule and could be

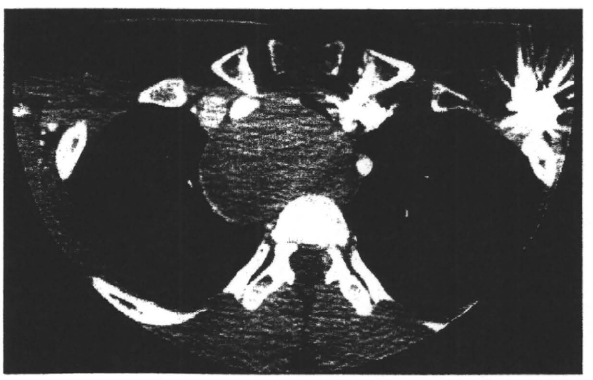

Fig 1. Computed tomographic scan of the thorax in the coronal plane. A large anterior mediastinal mass is demonstrated with maximum axial dimensions of 6.5 × 4.7 cm and craniocaudal extension of 7.6 cm. The trachea is significantly compressed measuring 5 mm in its mid-portion.

Accepted for publication Jan 13, 2010.

Address correspondence to Dr Halliday, Department of Cardiothoracic Surgery, Royal Infirmary of Edinburgh, 51 Little France Crescent, Old Dalkeith Rd, Edinburgh, EH16 4SA, United Kingdom; e-mail: jane.halliday@cantab.net.

Published by Elsevier Inc

0003-4975/$36.00
doi:10.1016/j.athoracsur.2010.01.083

Airway administration of dexamethasone, 3′-5′-cyclic adenosine monophosphate, and isobutylmethylxanthine facilitates compensatory lung growth in adult mice

Yusuke Takahashi, Yotaro Izumi, Mitsutomo Kohno, Masafumi Kawamura, Eiji Ikeda and Hiroaki Nomori

Am J Physiol Lung Cell Mol Physiol 300:L453-L461, 2011. First published 17 December 2010; doi:10.1152/ajplung.00100.2010

AJP - Lung Cellular and Molecular Physiology publishes original research covering the broad scope of molecular, cellular, and integrative aspects of normal and abnormal function of cells and components of the respiratory system. It is published 12 times a year (monthly) by the American Physiological Society, 9650 Rockville Pike, Bethesda MD 20814-3991. ISSN: 1040-0605, ESSN: 1522-1504. Visit our website at http://www.the-aps.org/.

Am J Physiol Lung Cell Mol Physiol 300: L453–L461, 2011.
First published December 17, 2010; doi:10.1152/ajplung.00100.2010.

Airway administration of dexamethasone, 3′-5′-cyclic adenosine monophosphate, and isobutylmethylxanthine facilitates compensatory lung growth in adult mice

Yusuke Takahashi,[1] Yotaro Izumi,[1] Mitsutomo Kohno,[1] Masafumi Kawamura,[1] Eiji Ikeda,[2] and Hiroaki Nomori[1]

[1]*Division of General Thoracic Surgery, Department of Surgery, School of Medicine, Keio University, Tokyo, Japan; and* [2]*Department of Pathology, Yamaguchi University Graduate School of Medicine, Yamaguchi, Japan*

Submitted 29 March 2010; accepted in final form 17 December 2010

Takahashi Y, Izumi Y, Kohno M, Kawamura M, Ikeda E, Nomori H. Airway administration of dexamethasone, 3′-5′-cyclic adenosine monophosphate, and isobutylmethylxanthine facilitates compensatory lung growth in adult mice. *Am J Physiol Lung Cell Mol Physiol* 300: L453–L461, 2011. First published December 17, 2010; doi:10.1152/ajplung.00100.2010.—The combination of dexamethasone, 8-bromo-3′-5′-cyclic adenosine monophosphate, and isobutylmethylxanthine, referred to as DCI, has been reported to optimally induce cell differentiation in fetal lung explants and type II epithelial cells. DCI administration is also known to modulate the expression levels of many genes known to be involved in the facilitation of lung growth. Recently, we found that RNA silencing of thyroid transcription factor 1 (TTF-1) delayed compensatory lung growth. DCI is also known to induce TTF-1 expression in pulmonary epithelial cells. From these findings, we hypothesized that DCI administration may facilitate compensatory lung growth. In the present study, using a postpneumonectomy lung growth model in 9-wk-old male mice, we found that compensatory lung growth was significantly facilitated by airway administration of DCI immediately following left pneumonectomy, as indicated by the increase in the residual right lung dry weight index. TTF-1 expression was significantly elevated by DCI administration, and transient knockdown of TTF-1 attenuated the facilitation of compensatory lung growth by DCI. These results suggested that DCI facilitated compensatory lung growth, at least in part, through the induction of TTF-1. Morphological analyses suggested that DCI administration increased the number of alveoli, made each of them smaller, and produced a net increase in the calculated surface area of the alveoli per volume of lung. The effect of a single administration was maintained during the observation period, which was 28 days. DCI with further modifications may provide the material to potentially augment residual lung function after resection.

thyroid transcription factor 1; wheel-running test; lung function

IT IS GENERALLY ACCEPTED IN the clinic that after lung resection in adults, the residual lung increases in volume to some extent, but that this increase is primarily hyperinflation with minimal recovery, and possibly even deterioration in lung function (16). In contrast, compensatory lung growth after lung resection has been reported in children (24) and in many animal models, including mice (7, 33). While this compensatory lung growth potential may be completely lost in the adult human lung, there is also evidence to suggest that the adult lung may, at least in part, regain its growth potential under certain conditions (5, 32) Developing research in tissue engineering and regeneration may some day accomplish the assembly of functional lung tissue ex vivo, but for the mean time, facilitation of compensatory lung growth in the residual lung may be a more attainable goal to improve residual lung function after resection.

The combination of dexamethasone (10 nM), 8-bromo-3′-5′-cyclic adenosine monophosphate (cAMP) (0.1 mM), and isobutylmethylxanthine (0.1 mM), referred to as DCI, has been reported to optimally induce cell differentiation in fetal lung explants and fetal lung cells (2, 8), as well as to maintain differentiation in already differentiated type II epithelial cells (3). The effects of DCI seem to be derived from the combination of dexamethasone and elevation of cAMP, but the exact mechanisms remain unclear.

DCI administration is known to modulate the expression levels of many genes in pulmonary epithelial cells. These include keratinocyte growth factor receptor and estrogen receptor (15), which have both been reported to be involved in the facilitation of lung growth in response to lung resection or various forms of lung injury. Recently, we found that RNA silencing of thyroid transcription factor 1 (TTF-1) delayed compensatory lung growth (31). DCI is also known to induce TTF-1 in pulmonary epithelial cells (15). From these findings, we hypothesized that DCI administration may facilitate compensatory lung growth. In the present study, using a mouse postpneumonectomy lung growth model, we observed the effects of DCI administration through the airway on compensatory lung growth.

MATERIALS AND METHODS

Animal experiments. Specific pathogen-free, 9-wk-old, inbred, male C57BL/6 mice, weighing ~20 g, were purchased from CLEA Japan, (Tokyo, Japan). The mice were kept in a 12:12-h light-dark cycle with free access to food and water.

The mice were randomly assigned to three experimental groups, left pneumonectomy (PNX) under mechanical ventilation followed by administration of DCI in Infasurf (PNX+DCI group), left pneumonectomy under mechanical ventilation followed by administration of Infasurf alone (PNX+INF group), or 9-wk-old male mice without any surgical interventions or treatment administration (NoTx group).

For left pneumonectomy, the mice were anesthetized with 100 mg/kg of ketamine and 10 mg/kg of xylazine administered subcutaneously. They were intubated with an 18-gauge catheter and connected to a rodent ventilator, adjusted to maintain a respiratory rate of 100 breaths/min, 10 ml/kg tidal volume, 2 cmH_2O positive end-expiratory pressure, and 0.21 inspired oxygen. A 20-mm-long postero-lateral skin incision was made, followed by thoracotomy in the fifth intercostal space with dissection of the serratus anterior and latissimus dorsi muscles. Left pneumonectomy was done by resecting the whole left lung from the pleural cavity. The left main bronchus with left pulmonary artery and vein were ligated at the hilum with a

Address for reprint requests and other correspondence: Y. Izumi, Division of General Thoracic Surgery, Dept. of Surgery, School of Medicine, Keio Univ., 35 Shinanomachi, Shinjuku-ku, Tokyo 160-8582, Japan (e-mail: yotaroizumi@a2.keio.jp).

5–0 silk suture before removal of the lung. The tidal volume was reduced from 10 to 6 ml/kg after the lung was removed. The fifth intercostal space was closed with a single surgical suture, and the skin and muscle incisions were closed with two sutures to avoid excessive tension on the muscles. The duration of mechanical ventilation for the whole surgical procedure was ~10 min. All mice recovered quickly after termination of mechanical ventilation and were promptly extubated.

After left pneumonectomy, DCI, a mixture of dexamethasone (500 ng/g; Sigma), 8-bromo-cAMP (5 μg/g; Santa Cruz Biotechnology, Santa Cruz, CA), and 3-isobutyl-1-methylxanthine (12.5 μg/g; Cal-

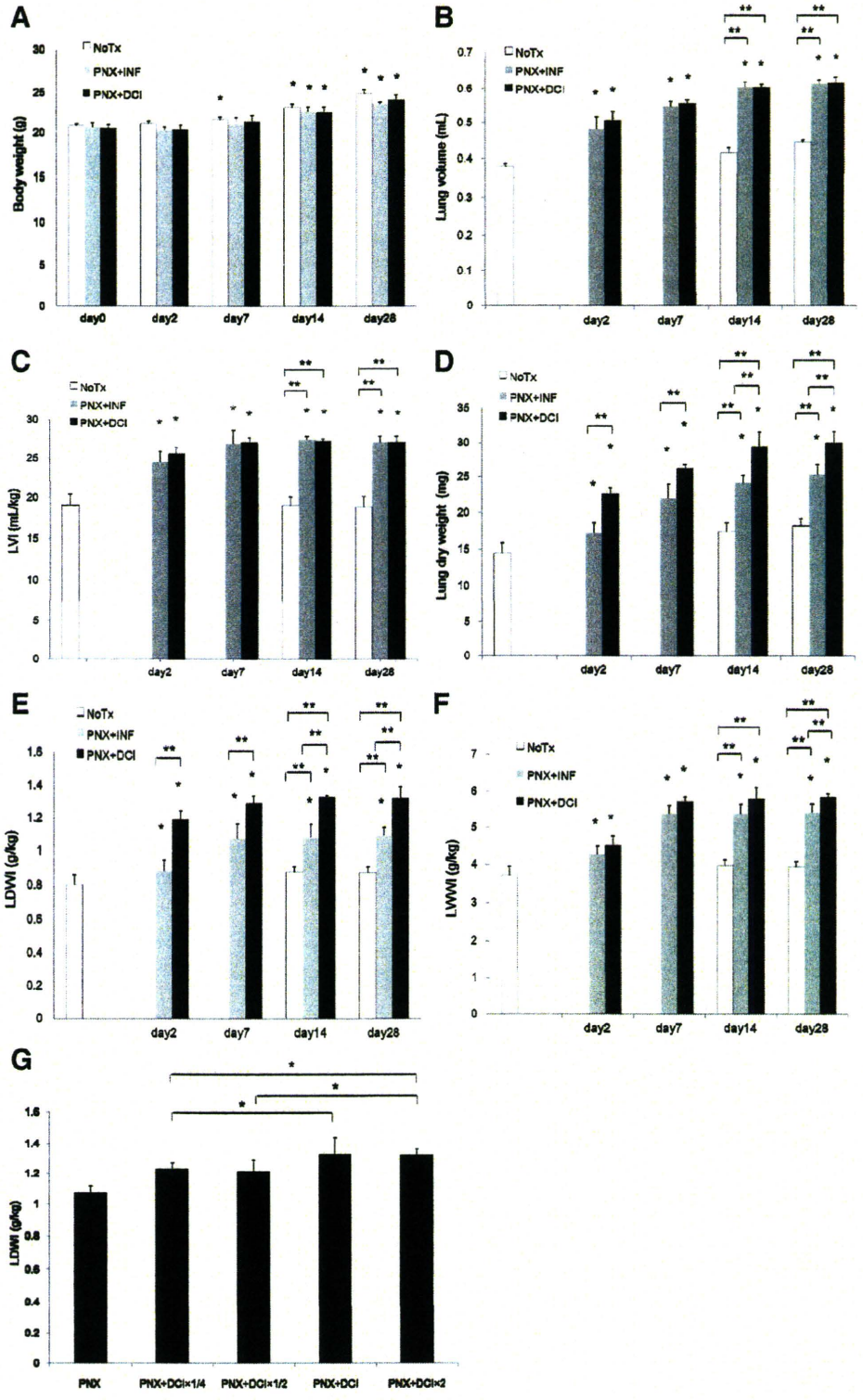

biochem, La Jolla, CA), was administered intranasally, as previously reported (18), with Infasurf (15 g/g; Ony, Amherst, New York) as a surface-active material (INF+DCI group). Infasurf alone was administered as a control (INF group). The in vivo dosage of DCI was extrapolated from the previously reported in vitro data (15), in vivo data (18, 36), and from our own experiences in the comparisons of in vitro vs. in vivo gene silencing using siRNAs. Administration into the nasal orifices was done using a microliter pipetter as a total of ~25 μl. The administration was done ~30 min after extubation in both groups, at which time the mice had sufficiently recovered breathing but were still immobilized. Nine-week-old male mice without any surgical interventions or treatment were also evaluated as NoTx group.

The mice were weighed and were observed daily for any signs of distress or changes in behavior. The mice were killed at indicated time points by injection of 100 mg/kg of ketamine and 10 mg/kg of xylazine, followed by exsanguination from the inferior vena cava. The right lung was resected at designated time points for histology or Western blot analysis, as described previously.

All experimental protocols were reviewed by the Committee on the Ethics of Animal Experiments at the School of Medicine, Keio University, and were carried out in accordance with Guidelines for Animal Experiments, issued by the School of Medicine, Keio University Experimental Animal Center.

Morphological analyses. For morphological analyses, the right lung was inflated with intratracheal instillation of 10% buffered formalin at a pressure of 20 cmH_2O. The trachea was tied under pressure, and the lung was fixed in the chest cavity for 48 h before removal. Total right lung volume was measured from the fixed specimen by volume displacement, as described by Scherle (29) as the lung volume (LV) and was also normalized to the body weight as lung volume index (LVI). The lung tissue was then embedded in paraffin and cut sagitally in 4-μm sections. Hematoxylin-and-eosin staining was done for histological analyses. Alveolus area was traced and calculated using Image J. Morphologically, alveoli were identified as polyhedral, cup, or wedged-shaped terminal air spaces with discrete septae, whereas terminal, somewhat elongated air spaces from which alveoli emerged, were considered as alveolar ducts (9). The alveolar surface area per unit of lung volume (SVw) was measured, as previously described by Weibel (34) and Kawakami et al. (10). Briefly, a standard line of the same length (LT) was drawn on the field, and intersections with this line were counted (Iw). SVw was calculated as SVw = 2 Iw/LT. For each analysis, one section was randomly selected per animal, and 5,200-fold magnification fields were randomly selected per section. The slides were coded and masked for identity and were examined by Y. Takahashi and E. Ikeda.

Lung weight measurements. The lung weight was measured as a gross assessment of compensatory lung growth. The resected lungs were lightly patted dry, weighed, and normalized to the body weight as the lung wet weight index (LWWI). The resected lungs were also completely dried in a vacuum drying oven (DP22; Yamato Scientific, Tokyo, Japan) at 95°C, and at −270 cmH_2O for 48 h, and then were weighed as the lung dry weight (LDW) and was also normalized to the body weight as the lung dry weight index (LDWI).

Transpulmonary pressure measurements. Transpulmonary pressures were measured in separate groups of animals by modifying previously reported methods (14, 30). The animals were killed by injection of 100 mg/kg of ketamine and 10 mg/kg of xylazine, followed by exsanguination from the inferior vena cava, 14 days after interventions in PNX (n = 5), PNX+INF (n = 5), and PNX+DCI (n = 5) groups. The animal was intubated, and the intubation tube was connected to an injection syringe and a water manometer (Innomedics Medical Instruments, Tokyo, Japan) by a three-way stopcock. The diaphragm was observed through the laparotomy. The lung was assumed to be at functional residual capacity after death, which was in agreement with the position of the diaphragm observed through the laparotomy. The lung was inflated by air at 0.1-ml increments, up to maximum inspiration observed by the position of the diaphragm, and then it was derecruited by deflation at 0.1 ml increments. Lung deflation was observed through the diaphragm. Intratracheal pressure during deflation was measured by the water manometer as the transpulmonary pressure. Static compliance was calculated as the slope of the curve from 0 to 5 cmH_2O of transpulmonary pressure.

Western blot analysis for TTF-1. For TTF-1 Western blot analysis, the right lung was resected at respective time points, blotted dry, immediately snap frozen in liquid nitrogen, and stored in −80°C. Western blot analysis for TTF-1 protein was performed according to a standard protocol. Briefly, lung tissue was lysed with a denaturing RIPA buffer (Sigma, Stockholm, Sweden), and the lysate was centrifuged at 14,000 rpm for 15 min at 4°C, and the supernatant was mixed with Laemmli buffer and applied to SDS-PAGE gels. The proteins were separated by 12.5% SDS-PAGE under reducing conditions and then transferred to PVDF membrane for 90 min at 90 V using HorizBlot system (ATTO, Tokyo, Japan). After blocking nonspecific reactions with Block Ace (Dainippon Pharmaceutical, Osaka, Japan), the primary antibody for TTF-1 (H-190: Santa Cruz Biotechnology, Santa Cruz, CA) and the antibody for β-actin (Abcam, Cambridge, UK) were incubated with the blot overnight at 4°C. The secondary anti-rabbit IgG: ECL anti-rabbit IgG horseradish peroxidase linked with whole antibody (GE Healthcare, Little Chalfont, Buckinghamshire, UK) was incubated with the blots for 1 h at room temperature.

Fig. 1. Changes in lung volume index and lung weight index after pneumonectomy and administration of a combination of dexamethasone, 8-bromo-3′-5′-cyclic adenosine monophosphate, and isobutylmethylxanthine (DCI). *A*: overall, the body weight of the mice was increased over time reflecting growth. The body weight of the mice was reduced in the left pneumonectomy (PNX)+DCI (n = 5) and PNX+ administration of Infasurf alone (INF; n = 5) groups compared with the NoTx (n = 5) group beyond *day 2*, but statistical significance was not reached. The body weight of the mice did not differ significantly between the PNX+DCI group and the PNX+INF group throughout the experiment period. *$P < 0.05$ vs. *day 0* of the same group. *B*: residual right lung volume index (LV) was increased significantly beyond *day 2* in both the PNX+DCI (n = 5 at each time point) group and the PNX+INF (n = 5 at each time point) group compared with the NoTx (n = 5 at each time point) group. Within the PNX+DCI group and the PNX+INF group, there were no statistically different increases beyond *day 2*. There was no statistical difference in LV between the PNX+DCI group and the PNX+INF group. *$P < 0.05$ vs. NoTx group. *C*: residual right lung volume index (LVI) was increased significantly beyond *day 2* in both the PNX+DCI (n = 5 at each time point) group and the PNX+INF (n = 5 at each time point) group compared with the NoTx (n = 5 at each time point) group. Within the PNX+DCI group and the PNX+INF group, there were no statistically different increases beyond day 2. There was no statistical difference in LVI between the PNX+DCI group and the PNX+INF group. *$P < 0.05$ vs. NoTx group. *D*: residual right lung dry weight (LDW) was significantly increased in the PNX+DCI (n = 5 at each time point) group compared with the PNX+INF (n = 5 at each time point) group and the NoTx (n = 5 at each time point) group beyond *day 2*. *$P < 0.05$ vs. NoTx group, **$P < 0.05$ between the indicated groups. *E*: residual right lung dry weight index (LDWI) was significantly increased in the PNX+DCI (n = 5 at each time point) group compared with the PNX+INF (n = 5 at each time point) group and the no treatment (NoTx; n = 5 at each time point) group beyond *day 2*. *$P < 0.05$ vs. NoTx group, **$P < 0.05$ between the indicated groups. *F*: residual right lung wet weight index (LWWI) tended to be higher in the PNX+DCI (n = 5) group compared with the PNX+INF (n = 5 at each time point) group and the NoTx (n = 5 at each time point) group beyond *day 2*. *$P < 0.05$ vs. NoTx group, **$P < 0.05$ between the indicated groups. *G*: LDWI at *day 14* was compared between different dosages of DCI (n = 5 in each group). One quarter, one half, and twofold amounts were administered. The twofold dose did not induce further increase in LDWI, while one-half or one-quarter dosage attenuated the increase in LDWI. Hence, the dosage used in this study was considered to be most suitable within the dosages evaluated. *$P < 0.05$ between the indicated groups.

Bands were detected by enhanced chemiluminescence using ECL Western blotting detection reagents (Amersham Bioscience, Piscataway, NJ). Band densitometry was quantified using Image J (National Institutes of Health, Bethesda, MD). Values were normalized to β-actin.

RNA silencing of TTF-1. TTF-1 silencing small inhibitory RNA oligoneucleotides, si#2 and si#4 (Invitrogen, Carlsbad, CA) were selected and administered as previously described (29). This method of administration has been shown to effectively reduce TTF-1 expression level in the lung after pneumonectomy. Sequences of si#2 and si#4 were (5′-UUGAAACGUCGCUCGAGCUCGUACA-3′) and (5′-GCUACAAGAUGAAGCGCCGGCUAA-3′), respectively. Thirty-five milligrams per kilogram of each inhibitory RNA was coadministered intranasally with DCI.

Exercise tests. Exercise function was tested using wheel-running tests (wheel circumference 75 cm) as an indirect index of lung function after pneumonectomy (23). Before each test, the mice were adapted to the wheel by ~200 rounds of voluntary wheel running. First, as an index of forced exercise, the mouse was placed on the wheel, and the wheel was manually spun at one round per second. This was continued until the mouse was unable to cope and was spun with the wheel, and the number of rounds was recorded. This was repeated 3 times with 5-min breaks in between, and was averaged. Next, after a 30-min break, as an index of semivoluntary exercise, the mouse was placed on the wheel, and the number of rounds spun in 5 min was recorded. The mouse was facilitated to run by touching on the tail if it stood still for longer than 5 s. Measurements were taken before pneumonectomy (*day 0*), and on *day 2*, *day 7*, and *day 14* after pneumonectomy and respective material administration. The NoTx group did not receive any treatment or surgery.

Statistical analysis. Data are expressed as means ± SD. Comparisons between groups were done using Mann-Whitney *U*-test (StatView; Abacus, Berkeley, CA). Body weight and exercise tests were compared within groups using paired *t*-test (StatView; Abacus). Other comparisons within groups were done using Mann-Whitney *U*-test since the animals were killed for respective time point measurements. *P* values less than 0.05 were considered to be statistically significant.

RESULTS

Lung volume and lung weight measurements. The body weight of the mice tended to increase within each group during the period of the experiment reflecting animal growth. It was reduced in the PNX+DCI (n = 5) and PNX+INF (n = 5) groups compared with the NoTx (n = 5) group beyond *day 2*, but statistical significance was not reached. The body weight of the mice did not differ significantly between the PNX+DCI group and the PNX+INF group throughout the experiment period (Fig. 1*A*). Therefore, it was considered feasible to compare weight-based indices between these groups.

The residual right LV and LVI were increased significantly beyond *day 2* in both the PNX+DCI (n = 5 at each time point) group and the PNX+INF (n = 5 at each time point) group compared with the NoTx (n = 5 at each time point) group. Within the PNX+DCI group and the PNX+INF group, there were no statistically different increases beyond *day 2*. There was no statistical difference between the PNX+DCI group and the PNX+INF group (Fig. 1, *B* and *C*).

In contrast to the changes in LV and LVI, the residual right LDW and LDWI was significantly increased in the PNX+DCI (n = 5 at each time point) group compared with the PNX+INF (n = 5 at each time point) group and the NoTx (n = 5 at each time point) group beyond *day 2* (Fig. 1, *D* and *E*). The magnitude of increase in LDWI in the PNX+INF group was similar to the previous data on left pneumonectomy alone (31). The LWWI also showed a similar tendency, although the difference between the PNX+DCI (n = 5 at each time point) group and the PNX+INF (n = 5 at each time point) reached statistical significance only on *day 28* (Fig. 1*F*).

The effect of DCI dosage on LDWI was also evaluated. The LDWI at *day 14* was compared between different dosages (n = 5 in each group) (Fig. 1*G*). The twofold dose did not induce further increase in LDWI, while one-half or one-quarter dosage attenuated the increase in LDWI. Hence, the dosage used in this study was considered to be most suitable within the dosages evaluated, at least in this particular model. DCI administration to mice without pneumonectomy did not induce any changes in LDWI.

Western blot analysis. Western blot analysis showed that TTF-1 expression in the residual right lung at *day 2* was significantly increased in the PNX+DCI group compared with pneumonectomy only (PNX group), the PNX+INF group or the NoTx group (Fig. 2*A*). We also concomitantly administered TTF-1 inhibitory RNAs (TTF-1 siRNAs) with DCI after pneumonectomy. The increase in LDWI by DCI administration was not affected by coadministration of TTF-1 siRNAs at *day 2* (n = 5 in each group) but was significantly suppressed at *day 7* by TTF-1 siRNAs (n = 5 in each group) (Fig. 2*B*).

Morphological analyses. On histology, the alveoli appeared to be smaller in the PNX+DCI group compared with the PNX+INF group or the NoTx group at *day 7* (Fig. 3*A*). Morphological analyses showed that the number of alveoli per field of view was significantly increased in the PNX+DCI group compared with the PNX+INF group and the NoTx group throughout the experiment (Fig. 3*B*). The average traced area of a single alveolus on histology was significantly decreased in the PNX+DCI group compared with the PNX+INF group and the NoTx group beyond 7 days (Fig. 3*C*). The traced total alveolar area per field was significantly increased in the PNX+DCI group compared with the PNX+INF group and the NoTx group beyond 2 days (Fig. 3*D*). The calculated surface area of the alveoli per volume of lung was also significantly increased in the PNX+DCI group compared with the PNX+INF group and the NoTx group at *day 28* (Fig. 3*E*).

Transpulmonary pressure measurements. The changes in transpulmonary pressure at *day 14* was not significantly different between PNX (n = 5), PNX+INF (n = 5), and the PNX+DCI (n = 5) groups (Fig. 4). The calculated static compliance was also not statistically different between groups [PNX, PNX+INF, and PNX+DCI groups, 186.8 ± 8.5, 190.8 ± 6.8, and192.4 ± 5.0, 10^{-3}ml/cm H_2O, respectively ($P > 0.05$)].

Exercise tests. General appearance, movement, and feeding behavior were similar between the PNX+DCI group and the PNX+INF group throughout the experiment period. Forced wheel running (n = 4 in each group) at *day 2* was significantly reduced in both groups compared with *day 0*. Recovery was seen beyond *day 7* in the PNX+DCI group but not in the PNX+INF group (Fig. 5*A*). Semivoluntary wheel running at *day 2* tended to be reduced in both PNX+DCI and PNX+INF groups compared with *day 0*. Recovery was seen at *day 7* in both groups without statistically significant differences. At *day 14*, the PNX+DCI group and the NoTx group showed significantly increased semivoluntary wheel running compared with their respective *day 0* values, presumably reflecting adaptation to wheel running, but the PNX+INF group remained at a similar level as *day 7*. The difference at *day 14* was significant between the PNX+DCI group and the PNX+INF group (Fig. 5*B*).